Measurement Back-Action and Photon Detection in Microwave Quantum Optics

ANTON FRISK KOCKUM

Department of Microtechnology and Nanoscience
Applied Quantum Physics Laboratory
CHALMERS UNIVERSITY OF TECHNOLOGY
Göteborg, Sweden 2012

Measurement Back-Action and Photon Detection
in Microwave Quantum Optics
ANTON FRISK KOCKUM

Thesis for the degree of Licentiate of Engineering

Cover: The time evolution of the coherent state in a resonator, dispersively coupled to a qubit, depending on the qubit state (green - qubit in the excited state, red - qubit in the ground state). The resonator is driven by a coherent signal, turned on at time $t = 0$ and turned off at time $t = t_{\mathrm{off}}$ (this is when the resonator states start spiralling back towards the origin). The figure is part of Paper I, and was selected to be part of the May 2012 "Kaleidoscope" of *Physical Review A*.

Measurement Back-Action and Photon Detection
in Microwave Quantum Optics

ANTON FRISK KOCKUM

Department of Microtechnology and Nanoscience
Applied Quantum Physics Laboratory
Chalmers University of Technology

Abstract

In quantum optics, the interaction between atoms and photons is studied. In recent years, microwave quantum optics with superconducting circuits has emerged as an important tool for fundamental quantum optics experiments, and also as a promising way for implementing quantum computation. The main reason for this development is the ease with which strong coupling and other properties of artificial atoms and microwave photons can be engineered in such a setup.

This thesis is comprised of two papers dealing with measurements in microwave quantum optics. In Paper I, we show how unwanted measurement back-action can be undone for certain measurements on one and two qubits dispersively coupled to a microwave resonator. An important application of this result is to improve parity measurements, which are integral to error-correction codes needed to implement large-scale quantum computing.

In Paper II, we investigate the possibility of using a three-level artificial atom, a transmon, to mediate a cross-Kerr type interaction between photons. The idea is to use it as a single-photon detector in the microwave regime, a component currently missing in the experimentalist's toolbox. We show that there are fundamental limitations to this setup, resulting in an unsatisfactory signal-to-noise ratio.

Keywords: Quantum Optics, Quantum Stochastic Calculus, Quantum Measurement, Transmon, Circuit QED, Photodetection, Parity Measurement, Dephasing

List of publications

I. **Undoing measurement-induced dephasing in circuit QED**
Anton Frisk Kockum, Lars Tornberg, and Göran Johansson
Physical Review A **85**, 052318 (2012)

II. **Breakdown of the cross-Kerr scheme for Photon Counting**
Bixuan Fan, Anton Frisk Kockum, Joshua Combes, Göran Johansson, Io-Chun Hoi, Christopher Wilson, Per Delsing, Gerard J. Milburn, and Thomas M. Stace
Submitted to *Physical Review Letters* (2012)
ArXiv preprint: arxiv.org/abs/1210.0991

Acknowledgements

First of all I would like to thank my supervisor Göran Johansson, for giving me the chance to work in the fascinating field of microwave quantum optics.

I owe big thanks to Lars Tornberg. You taught me the basics when I started out as a master student, and then returned to impart more knowledge to me as I continued as a PhD student. I really appreciate how you always seem available for fruitful discussions.

Thanks also to all the rest of the people in the Applied Quantum Physics Laboratory, and also in the Quantum Device Physics Laboratory, for making this such a fun and stimulating place to work.

I want to thank Bixuan Fan, and the rest of the people in Brisbane, for hosting me during my visit to University of Queensland. I look forward to our continued collaboration.

To Birger Jörgensen, and all the other great teachers who helped me reach this point.

Thanks to Göran, Lars, Anna, and Erik, for your helpful comments on the drafts of this thesis.

Thank you, friends and family, for your support and for all the good times we have shared.

Göteborg, November 2012
Anton Frisk Kockum

Contents

List of Figures

Chapter 1

Introduction

Quantum optics is the study of interaction between light and matter at a fundamental level, starting from individual atoms and photons. Experiments in the field provides an opportunity to test our understanding of the fascinating phenomena Nature provides at the quantum level. Prominent examples include the trapping, cooling, and probing of single atoms in ion traps [1], and the measurements of Schrödinger cat states in a microwave cavity probed by atoms [2], both of which were awarded the Nobel Prize in Physics 2012 [3].

1.1 Quantum optics on a chip

As technology has progressed, other experimental techniques for the study of quantum optics have been developed. One of the most promising is to use superconducting circuits on a chip to create artificial atoms that can be used as quantum bits, *qubits*. Here, transmission lines on the chip are used to guide microwave photons to control and read out the qubits. This approach, known as *circuit quantum electrodynamics* (circuit QED) [4, 5], has several advantages.

The fact that the system can be manufactured on a chip with lithographic methods allows for detailed design of properties suitable for the experiment in mind. The frequencies of the qubits, and the strength of their coupling to their surroundings can be set with good precision, and in some designs these important parameters can even be tuned *in situ*. There is also good potential to scale up the systems, which is needed to build a real quantum computer.

However, there are also drawbacks compared to other setups. The field of circuit QED is young compared to, *e.g.*, ion traps, and some tools available in experiments with optical photons are still missing. A prominent example is a good photodetector, which is more difficult to achieve for microwave photons as they have far less energy than optical photons.

In Paper II, we investigate the limits of a possible photodetection scheme in circuit QED. It's based on realizing a Kerr interaction using a three-level artificial atom. A photon, with frequency close to that of the first transition of the atom, is sent in along with a coherent probe signal, which has a frequency close to that of the second transition of the atom. The idea is that the atom mediates an interaction between the two, affecting the the probe signal differently depending on whether a signal photon is present or not.

1.2   Quantum computing and parity measurement

Ever since Feynman introduced the idea of a quantum computer [6], a computer which would harness the possibilities provided by Hilbert space, and quantum algorithms were shown to promise a great speed-up for solving certain problems [7, 8, 9, 10], there has been an ever-growing scientific community devoted to pursuing this goal.

In contrast to a classical computer, which operates on bits that are either 0 or 1, a quantum computer works with qubits. Qubits have eigenstates denoted $|0\rangle$ and $|1\rangle$, but they can be in any superposition of these states,

$$|\psi\rangle = \alpha|0\rangle + \beta|1\rangle, \tag{1.1}$$

where α and β are complex numbers satisfying $|\alpha|^2 + |\beta|^2 = 1$ [11]. This property allows for some computations to be carried out essentially in parallel, which gives the quantum computer its advantage over a classical computer.

While there has been considerable progress in the last years on implementing quantum computation using microwave quantum optics on a chip, the coherence time of the best qubits is still on the order of $0.1\,\text{ms}$ [12]. This is not enough to enable complicated computations with low enough error rate, but it is close to being useful for *quantum error correction codes*, where several qubits together represent and store the information of a single qubit (logical qubit). This redundancy allows for a kind of "majority

vote" system where if one qubit fails, that can be detected and corrected using the others.

In the last years, 2D *surface codes* have emerged as a good and scalable candidate for error correction in quantum computing [13, 14]. These and other codes use *parity measurements* to detect errors without disturbing the encoded logical qubit. A parity measurement on two or more qubits is a measurement which determines whether an even or odd number of them are in the same state. The measurement does not give any information about the states of the individual qubits. Thus, a parity measurement on two qubits tells us if they are in some superposition of $|00\rangle$ and $|11\rangle$ or in some superposition of $|01\rangle$ and $|10\rangle$. It does not give us any clue about whether the first qubit is in state $|0\rangle$ or $|1\rangle$.

The simple three-qubit code, which can protect against bit-flip errors, is a good example of how parity measurements can be used in error correction [11]. We encode the logical qubit state

$$|\Psi\rangle = \alpha|0\rangle + \beta|1\rangle, \tag{1.2}$$

using three qubits as

$$|\Psi\rangle_c = \alpha|000\rangle + \beta|111\rangle. \tag{1.3}$$

Now, let us assume that the third qubit is flipped. This gives

$$|\Psi\rangle_c = \alpha|001\rangle + \beta|110\rangle. \tag{1.4}$$

If we first do a parity measurement on qubits 1 and 2, and then on qubits 2 and 3, we do not affect the state $|\Psi\rangle_c$. However, the results of the measurements lets us draw the conclusion that qubit 3 has been flipped (assuming that the probability of more than one qubit flipping is negligible). We can then apply a control pulse to this qubit, flipping it back to its original state.

In Paper I, we show how parity measurements in circuit QED can be improved by undoing unwanted measurement back-action. The setup we investigate has two qubits coupled to a resonator. By driving the resonator with a coherent microwave signal, and detecting the output in a suitable way, one can for certain system parameters realize a parity measurement of the two qubits [15]. However, the measurement also seems to give extra back-action on one of the parity states, which would make it unsuitable for practical use. In our paper, we are able to show that a careful analysis of the measurement signal reveals all the information about this extra back-action needed to undo it.

1.3   Structure of the thesis

This thesis is structured as follows. In Chapter 2 we give a brief overview of some elements in circuit QED, the experimental implementation of microwave quantum optics with superconducting circuits. We cover transmission lines and transmon qubits, as they are the key elements in the possible experiments based on the two papers that are presented in this thesis.

The theoretical backbone of the thesis is found in Chapters 3 and 4. In Chapter 3, we go through the basics of input-output theory for quantum systems, and then develop the framework of stochastic master equations [16] to deal with how a system is affected by different kinds of measurements on its output. This formalism is a key ingredient in both Paper I and Paper II. We use the stochastic quantum calculus from Chapter 3 in Chapter 4 to provide a way of dealing with cascaded quantum systems, where the output from one system is used as the input for another. This is done by the (S,L,H) formalism [17, 18], which builds on the input-output theory of the previous chapter, and is used in both Paper I and Paper II. We also present a formalism for calculating the response of a system that is fed Fock state photons as an input [19]. This formalism is put to use in Paper II.

In Chapter 5, we give an overview of the most important results in Paper I and Paper II, and the methods used in obtaining them. We conclude by summarizing our results and looking to the future in Chapter 6.

Chapter 2

Circuit QED

There are several ways to do experiments in quantum optics. The archetypical setup is either single atoms (ions), trapped in an electromagnetic field, being manipulated with laser light [1, 3, 20, 21, 22], or the reverse, light trapped between two mirrors interacting with passing atoms [2, 3, 23, 24, 25]. In the last decade or so, an increasing number of quantum optics experiments have been done using superconducting circuits [4, 5, 26, 27, 28, 29]. The versatility offered by superconducting circuits in designing the "atoms" and their couplings to the surroundings, as well as the simplicity of using microwave signals for the photons, are the main reasons behind this development.

The work in both Paper I and Paper II is mainly done with an implementation using superconducting circuits in mind. Thus, this chapter will be devoted to introducing the main components used in quantum optics with superconducting circuits: the transmission line and the transmon. We will also say a few words about the Jaynes-Cummings model describing interaction between an atom and photons, and about the dispersive regime. We will not delve deeply into the process of quantizing the circuits, as this has already been well described elsewhere [30, 31, 32, 33, 34].

2.1   The transmission line

A transmission line can be modelled by the circuit depicted in Fig. 2.1 [35, 36]. To go from this circuit diagram to a quantum description, we first need to write down the Lagrangian $\mathfrak{L}$ [37] of the circuit. It turns out to be
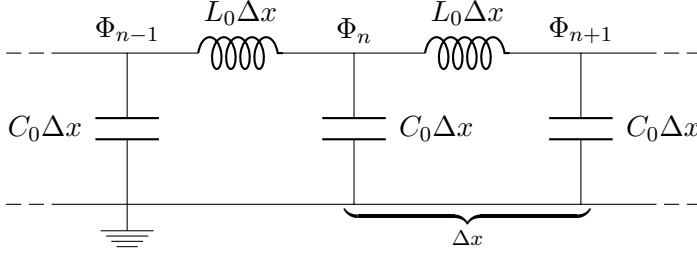
Figure 2.1: Circuit diagram for a transmission line. C_0 and L_0 denote capacitance per unit length and inductance per unit length, respectively.

convenient to work with node fluxes

$$\Phi(t) = \int_{-\infty}^{t} V(t')\,\mathrm{d}t', \tag{2.1}$$

where V denotes node voltage, and node charges

$$Q(t) = \int_{-\infty}^{t} I(t')\,\mathrm{d}t', \tag{2.2}$$

where I denotes node current. Using the node fluxes as our generalized coordinates, noting that the energy of a capacitor with capacitance C is $C\dot{\Phi}^2/2$ and the energy of an inductor with inductance L is $\Phi^2/(2L)$, we get the Lagrangian

$$\mathfrak{L} = \sum_{n} \left(\frac{1}{2} C_0 \Delta x \left(\dot{\Phi}_n(t) \right)^2 - \frac{1}{2 L_0 \Delta x} \left(\Phi_{n+1}(t) - \Phi_n(t) \right)^2 \right). \tag{2.3}$$

The Hamiltonian H now follows from the Legendre transformation [37]

$$H = \sum_{n} \frac{\partial \mathfrak{L}}{\partial \dot{\Phi}_n} \Phi_n - \mathfrak{L}, \tag{2.4}$$

where the generalized node momenta

$$\frac{\partial \mathfrak{L}}{\partial \dot{\Phi}_n} = C_0 \Delta x \dot{\Phi}(t) \tag{2.5}$$

can be identified as our node charges $Q_n(t)$. The Hamiltonian for the transmission line becomes, in the limit $\Delta x \to 0$,

$$H = \frac{1}{2} \int \left(\frac{Q(x,t)^2}{C_0} + \frac{1}{L} \left(\frac{\partial \Phi(x,t)}{\partial x} \right)^2 \right) \mathrm{d}x. \tag{2.6}$$

So far, everything has been done using classical mechanics. To make this description quantum mechanical, we promote $Q(x)$ and $\Phi(x)$ to operators with the canonical commutation relation

$$\big[\Phi(x), Q(x')\big] = i\hbar\delta(x - x'), \qquad (2.7)$$

where $\hbar$ is Planck's constant divided by 2π, and the delta function appears since we are working with a continuum model. This is the first and last time we will explicitly write out $\hbar$ in this thesis; in all of the following we will work in units where $\hbar = 1$.

The integrand in the Hamiltonian of Eq. (2.6) is familiar; it is that of a collection of coupled harmonic oscillators. We introduce creation and annihilation operators $a^\dagger(\omega)$ and $a(\omega)$, with commutation relation $\big[a(\omega), a^\dagger(\omega')\big] = \delta(\omega - \omega')$, in analogy with the procedure for a single harmonic oscillator [38]. Fourier expanding $Q(x)$ and $\Phi(x)$ in terms of these operators lets us rewrite the Hamiltonian as [33, 39]

$$H = \int_0^\infty \omega a^\dagger(\omega)a(\omega)\, \mathrm{d}\omega. \qquad (2.8)$$

Thus, we see that the transmission line supports a continuum of modes. It can be thought of as a "quantum wire" connecting quantum systems.

If part of a transmission line is terminated by capacitors or by connection to ground, it forms a resonator, the circuit equivalent of an optical cavity, which only supports a discrete number of modes. Usually the resonator is designed such that only the first mode (the one with the lowest frequency) comes into play, giving a simple harmonic oscillator with the Hamiltonian

$$H_{res} = \omega_r a^\dagger a, \qquad (2.9)$$

where $a^\dagger$ creates photons with frequency ω_r.

2.2   The transmon

There are several ways to build an artificial atom with superconducting circuits [40, 41, 42, 43, 44, 45]. Their common denominator is the use of *Josephson junctions* [46, 47] to provide a nonlinear element. In this section, we will give an overview of one implementation, the *transmon* [48], which is commonly used in circuit QED experiments today [12, 49, 50].
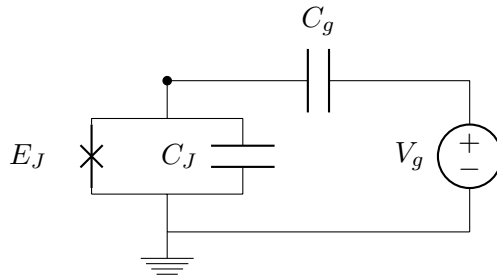
Figure 2.2: Circuit diagram for a Cooper pair box. The Josephson junction is modelled by the capacitance C_J in parallel with a tunnel barrier. The node between the gate capacitance C_g and the Josephson junction is called the "island".

The transmon is a *Cooper pair box* (CPB), the circuit diagram of which is shown in Fig. 2.2. The CPB consists of a small superconducting island connected to a superconducting reservoir via a Josephson junction, which allows Cooper pairs to tunnel on and off the island. The model also includes an external voltage source V_g coupled to the island via a capacitance C_g, to describe the number of Cooper pairs $n_g = C_g V_g / 2e$ (where e is the electron charge) that the environment induces on the island.

The Josephson junction is described by a capacitance C_J in parallel with a tunnel barrier that has energy $E_J(1 - \cos\phi)$, where E_J is called the Josephson energy of the junction, and $\phi = 2e\Phi$ is the phase across the junction [33, 47]. With this information we can write down the Lagrangian for the Cooper pair box,

$$\mathfrak{L}_{CPB} = \frac{C_g \left(\dot{\Phi} + V_g \right)^2}{2} + \frac{C_J \dot{\Phi}^2}{2} - E_J(1 - \cos 2e\Phi). \qquad (2.10)$$

Applying the Legendre transformation, identifying the conjugate momentum (the node charge) $Q = (C_g + C_J)\dot{\Phi} + C_g V_g$, and removing constant terms that do not contribute to the dynamics, we arrive at the Hamiltonian

$$H_{CPB} = 4E_C(n - n_g)^2 - E_J \cos\phi, \qquad (2.11)$$

where $E_C = e^2/2(C_g + C_J)$ is the electron charging energy, and $n = Q/2e$ is the number of Cooper pairs on the island.

We promote Φ and Q to operators in the same way as in the previous section. This translates into a commutation relation for n and ϕ, which

since the Hamiltonian is periodic in ϕ should be expressed as [34, 51]

$$\left[e^{i\phi}, n\right] = -e^{i\phi}. \tag{2.12}$$

From this we can derive $e^{\pm i\phi}|n\rangle = |n \pm 1\rangle$, where $|n\rangle$ is the charge basis counting the number of Cooper pairs. Using the resolution of unity [38] and $\cos\phi = (e^{i\phi} + e^{-i\phi})/2$ we can write the Hamiltonian as [32, 33]

$$H_{CPB} = \sum_n \left(4E_C(n - n_g)^2|n\rangle\langle n| - \frac{1}{2}E_J\Big(|n+1\rangle\langle n| + |n-1\rangle\langle n|\Big)\right) \tag{2.13}$$

The energy level structure of H_{CPB} depends on the parameters E_J, E_C and n_g. As n_g represents the influence of the environment, we would like it to have small influence in order to have a stable system. It turns out that this is achieved when $E_J/E_C \gg 1$, as is illustrated in Fig. 2.3. The price to be paid is a decrease in *anharmonicity*, *i.e.*, the difference between the energy needed to go from the ground state to the first excited state and the energy needed to go from the first excited state to the second excited state. To work as a qubit, an artificial atom has to be anharmonic enough to be approximated as a two-level system when driving the first transition, *i.e.*, a signal driving a transition from the ground state to the first excited state shouldn't be able to induce a further transition to the second excited state. Fortunately, it turns out that the anharmonicity is enough for the transmon in the limit $E_J/E_C \gg 1$, so it can be used as a qubit. In some cases, however, the second excited state is actually used to implement multi-qubit gates [50, 52].

2.3   The Jaynes-Cummings model and the dispersive regime

An important and common setup in quantum optics is that of one or several atoms coupled to a resonator. An illustration of how this can be implemented in circuit QED for two transmons and a transmission line resonator is shown in Fig. 2.4. The system consisting of a resonator and one two-level atom (qubit) can be described by the *Rabi Hamiltonian* [53]

$$H_R = \omega_r a^\dagger a + \frac{\omega_0}{2}\sigma_z + g\sigma_x\left(a + a^\dagger\right), \tag{2.14}$$

where ω_r is the frequency of the resonator, ω_0 is the frequency of the qubit, g is the strength of the coupling between the qubit and the resonator, a
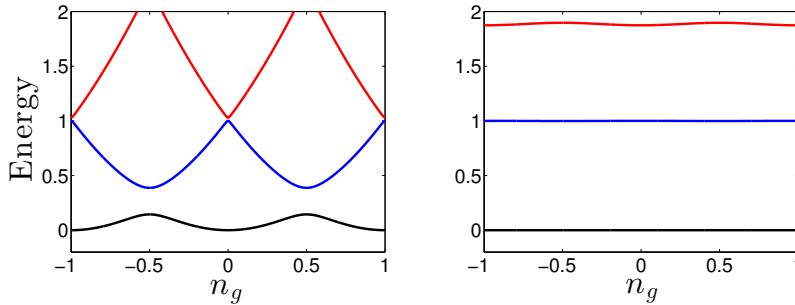
Figure 2.3: The three lowest energy levels of a CPB plotted as a function of n_g for $E_J/E_C = 1$ (left) and $E_J/E_C = 20$ (right). The energy scale is normalized to the level separation between the ground state and the first excited state at $n_g = 0$. The decreased sensitivity to charge noise in the transmon regime, $E_J/E_C \gg 1$, as well as the decreased anharmonicity, is apparent.
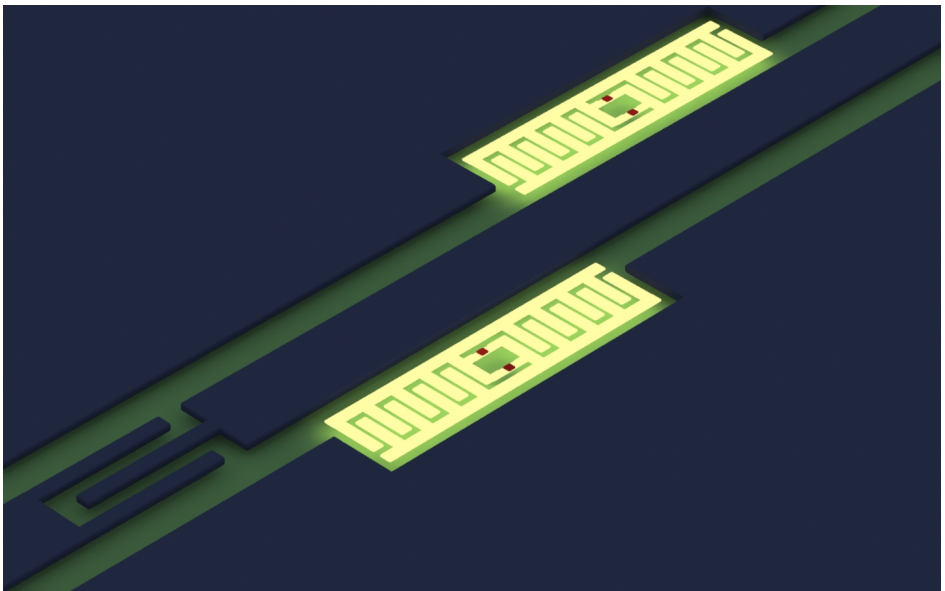
Figure 2.4: An artist's rendering of a transmission line resonator coupled to two transmons. The dark blue line in the center is the center conductor of the transmission line, interrupted by a capacitance to the left. The large dark blue areas are ground planes. The golden sawtooth shapes form the large capacitances of the two transmons (needed to achieve $E_J/E_C \gg 1$), and the red dots are the Josephson junctions (two junctions, instead of one, are used in a SQUID configuration [48] to allow tuning of E_J with an external magnetic field). Illustration by Philip Krantz (www.krantznanoart.com).

$(a^\dagger)$ is the annihilation (creation) operator for the resonator mode, and the σ_i are Pauli matrices describing the qubit. σ_x can be rewritten as $\sigma_- + \sigma_+$, where σ_- (σ_+) is the lowering (raising) operator of the qubit.

In the last part of Eq. (2.14) we have the terms $a\sigma_-$ and $a^\dagger\sigma_+$, which will oscillate with frequency $\omega_r + \omega_0$ in the interaction picture. If this frequency is much larger than g, these terms will average out and we can neglect them in our calculations. This is known as the *rotating wave approximation* (RWA). It reduces the Rabi Hamiltonian to the *Jaynes-Cummings model* [51, 54],

$$H_{JC} = \omega_r a^\dagger a + \frac{\omega_0}{2}\sigma_z + g\left(a\sigma_+ + a^\dagger\sigma_-\right). \tag{2.15}$$

In this model, the number of excitations in the system is conserved, allowing for an explicit solution of the Hamiltonian. It is straightforward to extend this model to include more than two levels of the atom, as is sometimes needed when dealing with a transmon [48], or to include more atoms [55]. The only added complication is that the photons don't couple equally strongly to all level transitions.

A useful twist on the Jaynes-Cummings model is the *dispersive regime*, which is when the *detuning* $|\Delta| = |\omega_0 - \omega_r|$ is much larger than the coupling strength g. In this case, we can apply the unitary transformation

$$U_{disp} = \exp\left[\lambda\left(a^\dagger\sigma_- - a\sigma_+\right)\right], \tag{2.16}$$

where $\lambda = g/\Delta$, to Eq. (2.15), and do a perturbation expansion in the small parameter λ. Keeping terms up to first order in λ gives

$$H_{disp} = \left(\omega_r + \chi\sigma_z\right)a^\dagger a + \frac{\omega_0 + \chi}{2}\sigma_z, \tag{2.17}$$

where $\chi = g^2/\Delta$. Perturbation expansion to higher order in λ is possible [56], and the procedure can also be carried out for a multi-level atom [48].

The most important feature of the Hamiltonian in Eq. (2.17) is that the qubit and the resonator no longer interact by exchanging excitations. Instead, changing the state of the qubit will effectively shift the resonator frequency, and changing the number of photons in the resonator will effectively shift the qubit frequency. Both these properties have been used to do *quantum non-demolition* (QND) measurements of qubit states [5, 57] and photon number [23, 58]. The measurements we consider in Paper I are all based on using a coherent signal to probe a resonator dispersively coupled to one or two qubits.

Another advantage of the dispersive regime is that it allows us to trace out the resonator degrees of freedom to achieve an effective description for just the qubit. This procedure is an integral part of Paper I. It reduces the number of degrees of freedom in the system from infinity to 2, and lets us see clearly what back-action a measurement on the resonator has on the qubit.

In this section, we considered coupling a transmon to a transmission line resonator. It is also possible to dispense with the capacitors at the ends of the resonator and couple the transmon directly to the continuum of modes in the open transmission line. This is the setup we employ in Paper II. However, to properly discuss it we need to take a closer look at *open quantum systems*, *i.e.*, quantum systems that are coupled to a surrounding environment. This is part of the topic for the next chapter.

Chapter 3

Stochastic Master Equations

For a *closed quantum system*, a system which does not interact in any way with the surroundings, the Hamiltonian H of the system gives us all the information we need. We can either describe the dynamics in the *Schrödinger picture*, where the state of the system, $|\psi\rangle$, evolves in time according to the *Schrödinger equation* [38]

$$\frac{\mathrm{d}}{\mathrm{d}t}|\psi\rangle = -iH|\psi\rangle, \tag{3.1}$$

and system operators are constant, or in the *Heisenberg picture*, where the state is constant and a system operator a evolves according to the *Heisenberg equation* [38]

$$\dot{a} = -i\left[a, H\right]. \tag{3.2}$$

Another, more general, way to describe the state and its evolution in the Schrödinger picture is to use the density matrix ρ. The time evolution for ρ is given by the *Liouville - von Neumann equation*

$$\dot{\rho} = -i\left[H, \rho\right], \tag{3.3}$$

which is easily derived from the Schrödinger equation [38]. The density matrix representation is the most convenient one when we open up the system to influence from the outside. Let us assume our system is a harmonic oscillator with annihilation operator a. If this system is linearly coupled to a bath of harmonic oscillators (a typical model for an environment), it can be shown, under some reasonable assumptions which we will discuss in the next section, that the Liouville-von Neumann equation for

the system density operator ρ is modified to [59, 60, 61]

$$\dot{\rho} = -i\left[H, \rho\right] + \kappa \mathcal{D}\left[a\right]\rho, \tag{3.4}$$

where $\mathcal{D}\left[a\right]\rho = a\rho a^{\dagger} - \frac{1}{2}a^{\dagger}a\rho - \frac{1}{2}\rho a^{\dagger}a$, and κ is the relaxation rate, the rate at which photons leak out from the system. This is called a *master equation* on the *Lindblad form* [62]. Having the master equation on this form ensures that the density matrix properties $\rho = \rho^{\dagger}$, $\text{tr}\left(\rho\right) = 1$, and $\rho > 0$ are preserved.

Given ρ and its time evolution the expectation value of a system operator b is obtained from $\langle b \rangle = \text{tr}\left(b\rho\right)$, and the time evolution of this expectation value becomes $\partial_t \langle b \rangle = \text{tr}\left(b\dot{\rho}\right)$.

The formalism above, though useful for understanding what happens in an open quantum system, does not yet allow us to make statements about what the output from the system to the surroundings is. To remedy this we will therefore in this chapter look at *input-output theory* [61, 63]. Furthermore, we will investigate what happens when a measurement is done on the output signal, and what kind of back-action this can give on the system. This will give us the framework of *stochastic master equations* (SMEs) [16], which is employed in both papers of this thesis. For the next chapter we leave the topic of how to deal with cascaded quantum systems, *i.e.*, a series of systems where the output from one is used as input to another.

3.1   Input-output theory

Let us have a closer look at the example, mentioned above, of a harmonic oscillator (the system) coupled to an environment. The system has the Hamiltonian

$$H_{\text{sys}} = \omega_s a^{\dagger}a, \tag{3.5}$$

where ω_s is the oscillator frequency. The environment is modelled as a collection of harmonic oscillators, an electromagnetic field if you will, with Hamiltonian

$$H_{\text{env}} = \int_0^{\infty} \omega b^{\dagger}(\omega)b(\omega)\,\mathrm{d}\omega, \tag{3.6}$$

and the coupling between system and environment is given by

$$H_{\text{int}} = i\int_0^{\infty} \sqrt{\frac{\kappa(\omega)}{2\pi}}\left(b^{\dagger}(\omega)a - a^{\dagger}b(\omega)\right)\,\mathrm{d}\omega, \tag{3.7}$$

where $\kappa(\omega)$ is some frequency-dependent coupling strength. To get this interaction we made the RWA, *i.e* we assumed that terms like $ab(\omega)$ oscillate rapidly and average out on the timescales we are interested in, just like when we went from Eq. (2.14) to Eq. (2.15) in Section 2.3.

To study input and output for the system we follow Ref. [63]. We begin by extending the integration limits to $-\infty$ in Eq. (3.6) and Eq. (3.7). This is an acceptable approximation, since only terms with frequencies close to ω_s are important. With this modification done, we write down the Heisenberg equation for the system and field operators. Using the commutation relations $\left[a, a^\dagger\right] = 1$ and $\left[b(\omega), b^\dagger(\omega')\right] = \delta(\omega - \omega')$ gives

$$\dot{b}(\omega) = -i\omega b(\omega) + \sqrt{\frac{\kappa(\omega)}{2\pi}} a, \tag{3.8}$$

$$\dot{a} = -i\omega_s a - \int_{-\infty}^{\infty} \sqrt{\frac{\kappa(\omega)}{2\pi}} b(\omega) \, \mathrm{d}\omega. \tag{3.9}$$

Defining $b_0(\omega) = b(\omega, t = t_0)$ as the initial field state at some time $t_0 < t$ lets us write the solution to the first equation as

$$b(\omega) = e^{-i\omega(t-t_0)} b_0(\omega) + \sqrt{\frac{\kappa(\omega)}{2\pi}} \int_{t_0}^{t} a(t') e^{-i\omega(t-t')} \, \mathrm{d}t. \tag{3.10}$$

Now, we make the *Markov approximation* that $\kappa(\omega)$ varies slowly around ω_s and thus can be taken to be constant, $\kappa(\omega) = \kappa$. This gives the idealized description of white noise, which is delta-correlated (the damping of the system at time t will only depend on the field at time t, not on the field at any previous time). We also define the *in-field*

$$b_{in}(t) = \frac{1}{\sqrt{2\pi}} \int_{-\infty}^{\infty} e^{-i\omega(t-t_0)} b_0(\omega) \, \mathrm{d}\omega. \tag{3.11}$$

Inserting the expression for $b(\omega)$ from Eq. (3.10) into Eq. (3.9) with this addition gives, after a little algebra, that the equation for a can be written

$$\dot{a} = -i\omega_s a - \sqrt{\kappa} b_{in}(t) - \frac{\kappa}{2} a. \tag{3.12}$$

From this we see two things. Firstly, the in-field will affect the evolution of the system operator a. Secondly, even if there is no input from the field the coupling will still give rise to damping of a.

Another way to solve the Heisenberg equation for $b(\omega)$ is to define $b_1(\omega) = b(\omega, t = t_1)$ as the future field state at some time $t_1 > t$. This gives

$$b(\omega) = e^{-i\omega(t-t_1)}b_1(\omega) - \sqrt{\frac{\kappa(\omega)}{2\pi}} \int_t^{t_1} a(t')e^{-i\omega(t-t')}\,\mathrm{d}t, \qquad (3.13)$$

and defining the out-field

$$b_{out}(t) = \frac{1}{\sqrt{2\pi}} \int_{-\infty}^{\infty} e^{-i\omega(t-t_1)}b_1(\omega)\,\mathrm{d}\omega \qquad (3.14)$$

lets us write the time-reversed equation for a as

$$\dot{a} = -i\omega_s a - \sqrt{\kappa}b_{out}(t) + \frac{\kappa}{2}a. \qquad (3.15)$$

Using that Eq. (3.12) and Eq. (3.15) should give the same result at time t now gives the important result

$$b_{out}(t) = b_{in}(t) + \sqrt{\kappa}a(t), \qquad (3.16)$$

which connects input and output, the goal of this section.

3.2   Measurement back-action - an example

Before we move on to deriving SMEs for different types of measurements, let us study a simple example of measurement back-action which will prove illuminating for the discussion in Paper I. Imagine we have a system consisting of a qubit in a state

$$|\Psi\rangle_s = \alpha|0\rangle + \beta|1\rangle. \qquad (3.17)$$

We now want to do a measurement on this system. However, we don't do a direct projective measurement on the qubit. Instead we send in a second qubit, a probe, which becomes entangled with the system. We then do a measurement on the probe qubit and see what this lets us infer about the system qubit.

The simplest version of this protocol is when the two qubits become fully entangled, giving a state for system+probe

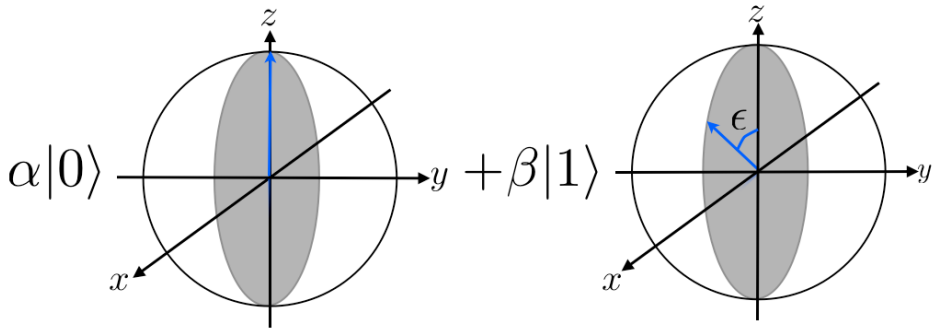$$|\Psi\rangle_{s+p} = \alpha|00\rangle + \beta|11\rangle. \qquad (3.18)$$

Figure 3.1: The weakly entangled state illustrated using the Bloch sphere representation for the probe qubit. The north and south poles of the sphere correspond to the states $|0\rangle$ and $|1\rangle$, respectively. Illustration by Lars Tornberg.

Measuring the probe qubit to be in state $|1\rangle$ ($|0\rangle$) will then project the system qubit into state $|1\rangle$ ($|0\rangle$). In other words, the act of measuring the probe qubit gives *back-action* on the system qubit.

There are two ways to get more interesting back-action. Firstly, we can choose to measure the probe qubit in some other basis (above we measured in the Z basis). Secondly, the entanglement can be weaker. Let us study a weakly entangled state

$$|\Psi\rangle_{s+p} = \alpha|00\rangle + \beta|1\rangle \left(\cos\frac{\epsilon}{2}|0\rangle + \sin\frac{\epsilon}{2}|1\rangle\right), \qquad (3.19)$$

pictured in Fig. 3.1. If we now measure the probe qubit in the Z basis we get

$$|\Psi\rangle_s = \begin{cases} \frac{\alpha|0\rangle + \beta\cos\epsilon/2|1\rangle}{\sqrt{|\alpha|^2 + |\beta|^2\cos^2\epsilon/2}}, & \text{if } Z = +1, \\ |1\rangle, & \text{if } Z = -1, \end{cases} \qquad (3.20)$$

That is, measuring $Z = +1$ only gives us a little information about the system qubit if ϵ is small, and in turn the back-action of the measurement is small. If we look at the probe qubit in the Y basis instead we find

$$|\Psi\rangle_s = \begin{cases} \alpha|0\rangle + \beta e^{i\epsilon/2}|1\rangle, & \text{if } Y = +1, \\ \alpha|0\rangle + \beta e^{-i\epsilon/2}|1\rangle, & \text{if } Y = -1, \end{cases} \qquad (3.21)$$

Here we see that the measurement does not give any information about the chances of finding the system qubit in state $|0\rangle$ or $|1\rangle$, since the probabilities

for the Y measurement results do not depend on α and β. However, there was still a measurement back-action in the form of a phase kick to the system qubit. Also, if we know the degree of entanglement ϵ we know what the measurement back-action was given the measurement result.

This last example is closely connected to our observations in Paper I. There, we send in photons which become entangled with a system qubit. Measuring the photons in one way gives information about the qubit state, but measuring them another way only gives rise to a measurement back-action in the form of phase kicks which can be calculated and undone given the measurement record.

3.3   Measurements and stochastic calculus

In the example above, we arrived at the final state of the system, conditioned on the measurement result, by projecting into the subspace corresponding to the measurement result and then tracing out the probe. In general, we consider the time evolution of a density matrix

$$\rho(t) = U(t)\rho(0)U^\dagger(t) \tag{3.22}$$

for the combined Hilbert space of the system and the probe. Here $U(t) = U(t,0)$ is the time evolution operator.

The measurement can give different outcomes i, corresponding to projecting the probe into the state $|i\rangle$ in the Hilbert space of the probe. The probability of outcome i is $p_i = \mathrm{tr}\left(|i\rangle\langle i|\rho|i\rangle\langle i|\right)$. If we assume that the probe is initialized in some ground state $|0\rangle$, then the system density matrix, after the measurement shows result i, is given by

$$\rho_i^s(t) = \frac{1}{p_i}\left\langle i \left| U(t)(\rho^s(0) \otimes |0\rangle\langle 0|)U^\dagger(t) \right| i \right\rangle = \frac{1}{p_i}\Omega_i(t)\rho^s(0)\Omega_i^\dagger(t). \tag{3.23}$$

Here we define the operator $\Omega_i(t) = \langle i\left| U(t) \right| 0\rangle$, which is an operator living in the system Hilbert space. This allows us to rewrite the expression for the probability: $p_i(t) = \mathrm{tr}\left(\Omega_i(t)\rho^s\Omega_i^\dagger(t)\right)$.

Assuming the measurement takes place during some short time $\mathrm{d}t$ we arrive at the equation of motion for the system density matrix [11, 32],

$$\rho_i(t + \mathrm{d}t) = \frac{1}{p_i(\mathrm{d}t)}\Omega_i(\mathrm{d}t)\rho_i(t)\Omega_i^\dagger(\mathrm{d}t). \tag{3.24}$$

It is important to note that this is very different from the master equation presented in the first section of this chapter, as we now have allowed for measurements, which means that probabilities come into play and turns this into a *stochastic* equation. An equation of this type, which gives the evolution of a system conditioned on measurements, is often referred to as a *quantum trajectory equation* [64, 65]. While a usual master equation describes the average evolution of a system over many experiments, a quantum trajectory is like a single run of an experiment. Thus, averaging over the possible measurement outcomes will let us recover the usual master equation from a quantum trajectory equation, which we will see examples of later on.

We will in the following sections derive stochastic master equations for photodetection and homodyne detection. To make this task (and also the calculations of the next chapter) easier, we will first develop some notation and concepts from the section on input-output theory. There, in Section 3.1, we defined the in-field $b_{in}(t)$. Setting $t_0 = 0$ for simplicity from here on, we can calculate the commutation relation

$$
\begin{aligned}
\left[b_{in}(t), b_{in}^\dagger(t')\right] &= \frac{1}{2\pi} \int_{-\infty}^{\infty} \mathrm{d}\omega \int_{-\infty}^{\infty} \mathrm{d}\omega' e^{-i\omega t + i\omega' t'} \left[b_0(\omega), b_0^\dagger(\omega)\right] \\
&= \frac{1}{2\pi} \int_{-\infty}^{\infty} \mathrm{d}\omega e^{-i\omega(t-t')} = \delta(t - t'),
\end{aligned}
\tag{3.25}
$$

which strengthens the view of $b_{in}(t)$ as white noise. We define [61, 63]

$$
B_t = \int_0^t b_{in}(s)\,\mathrm{d}s,
\tag{3.26}
$$

which is known as a *quantum Wiener process*. From this we get the *quantum noise increments*

$$
\mathrm{d}B_t = \int_t^{t+\mathrm{d}t} b_{in}(s)\mathrm{d}s,
\tag{3.27}
$$

which is often written on differential form as $\mathrm{d}B_t = b_{in}(t)\mathrm{d}t$.

Now we are ready to write down the time evolution operator $U(t)$, which we will need to calculate the effect of measurements. Moving to the

rotating frame of H_{env} we have

$$
\begin{aligned}
U(t) &= \mathcal{T} \exp\left[-i \int_0^t \mathrm{d}t' \Big(H_{sys} \right. \\
&\qquad\qquad \left. +i\sqrt{\frac{\kappa}{2\pi}} \int \mathrm{d}\omega \left(ab^\dagger(\omega)e^{i\omega t'} - a^\dagger b(\omega)e^{-i\omega t'} \right) \Big) \right] \\
&= \mathcal{T} \exp\left[-iH_{sys}t + \sqrt{\kappa}\left(aB_t^\dagger - a^\dagger B_t \right) \right],
\end{aligned}
\tag{3.28}
$$

where $\mathcal{T}$ is the time-ordering operator. Note that we here have replaced the b's with b_0's to get the final result. This can be done since

$$
\int_{-\infty}^{\infty} \mathrm{d}\omega\, b(\omega) = b_{in}(t) + \frac{\sqrt{\kappa}}{2} a(t),
\tag{3.29}
$$

and the term with $a(t)$ will only give rise to a constant when Eq. (3.29) is inserted into the coupling Hamiltonian Eq. (3.7). A constant term in the Hamiltonian does not affect the dynamics, and can thus be ignored.

We would like to expand Eq. (3.28) for a small increment in t to get $\mathrm{d}U_t$. However, care is required when dealing with stochastic increments. There are two approaches to the problem: *Stratonovich calculus* and *Itō calculus* [61, 63, 66, 67, 68].

In Stratonovich calculus, an integral of some function or system operator $f(t)$ with stochastic increments is defined as

$$
\int_0^t f(t')\, \mathrm{d}B_{t'} = \lim_{n\to\infty} \sum_{i=0}^{n} \frac{1}{2}\left(f(t_i) + f(t_{i+1}) \right)\left(B_{t_{i+1}} - B_{t_i} \right).
\tag{3.30}
$$

The advantage with this approach is that the chain rule of ordinary calculus continues to hold for stochastic increments, *i.e.*, $\mathrm{d}(AB) = A(\mathrm{d}B) + (\mathrm{d}A)B$ even for stochastic processes A and B. The downside is that the terms in the sum defining the integral don't necessarily commute, as the terms are defined on overlapping time intervals.

In Itō calculus, the same integral is instead defined as

$$
\int_0^t f(t')\, \mathrm{d}B_{t'} = \lim_{n\to\infty} \sum_{i=0}^{n} f(t_i)\left(B_{t_{i+1}} - B_{t_i} \right),
\tag{3.31}
$$

which ensures that the terms in the sum commute, as they only overlap on a time interval of length zero ($f(t_i)$ only depends on B_t with $t < t_i$).

The prize to pay is that the chain rule has to be modified to $d(AB) = A(dB) + (dA)B + (dA)(dB)$. In the following we will work with Itō calculus, since the fact that $f(t') \, dB_{t'}$ commute makes calculating expectation values easier.

Before we can find dU_t, we need to calculate expectation values like

$$
\begin{aligned}
\left\langle dB_t dB_t^\dagger \right\rangle &= \int_t^{t+dt} dt' \int_t^{t+dt} dt'' \left\langle 0 \left| b_{in}(t') b_{in}^\dagger(t'') \right| 0 \right\rangle \\
&= \int_t^{t+dt} dt' \int_t^{t+dt} dt'' \left\langle 0 \left| \left[b_{in}(t'), b_{in}^\dagger(t'') \right] \right| 0 \right\rangle \\
&= \int_t^{t+dt} dt' \int_t^{t+dt} dt'' \delta(t' - t'') \langle 0|0 \rangle \\
&= \int_t^{t+dt} dt' = dt,
\end{aligned} \tag{3.32}
$$

where we have used $b_{in}(t)|0\rangle = 0$ in the first equality. This tells us that under vacuum expectations we can treat $dB_t dB_t^\dagger$ as dt. Similar calculations give that $dB_t dB_t$, $dB_t^\dagger dB_t^\dagger$, and $dB_t^\dagger dB_t$ are all 0. These are known as the Itō rules for vacuum expectations, and they show why B_t is called a quantum Wiener process. The Itō rules can be generalized to having the bath in a thermal state [61, 63].

Expanding Eq. (3.28) using Itō calculus now gives

$$
\begin{aligned}
dU_t &= \Big[-iH_{sys}dt + \sqrt{\kappa} \left(a dB_t^\dagger - a^\dagger dB_t \right) \\
&\quad + \frac{1}{2} \left(-iH_{sys}dt + \sqrt{\kappa} \left(a dB_t^\dagger - a^\dagger dB_t \right) \right)^2 + \mathcal{O}(t^{3/2}) \Big] U_t \\
&= \Big[-iH_{sys}dt + \left(L dB_t^\dagger - L^\dagger dB_t \right) - \frac{1}{2} L^\dagger L dt + \mathcal{O}(t^{3/2}) \Big] U_t, \tag{3.33}
\end{aligned}
$$

where we have introduced the common notation $L = \sqrt{\kappa} a$. With this expression for the time evolution we can now also derive the *Itō Langevin equation* for a system operator c [61, 63],

$$
\begin{aligned}
dc(t) &= d(U_t^\dagger c U_t) = dU_t^\dagger c U_t + U_t^\dagger c dU_t + dU_t^\dagger c dU_t \\
&= -i \left[c(t), H_{sys}(t) \right] dt + \mathcal{D}^\dagger[L(t)] c(t) dt \\
&\quad + [c(t), L(t)] \, dB_t^\dagger + \left[L^\dagger(t), c(t) \right] dB_t, \tag{3.34}
\end{aligned}
$$

where $\mathcal{D}^\dagger[L]c = L^\dagger c L - \frac{1}{2} \{ L^\dagger L, c \}$, and we have used the Itō rules for vacuum expectations.

To calculate expectation values of system operators, we can either stay in the Heisenberg picture and use Eq. (3.34), or we can find an effective density matrix for the system in the Schrödinger picture. To do the latter, we note that

$$
\begin{aligned}
\langle c(t) \rangle &= \mathrm{tr}_S \mathrm{tr}_B \left[(c(t) \otimes \mathbf{1}_B) \left(\rho_S(0) \otimes \rho_B(0) \right) \right] \\
&= \mathrm{tr}_S \mathrm{tr}_B \left[U^\dagger(t) \left(c(0) \otimes \mathbf{1}_B \right) U(t) \left(\rho_S(0) \otimes \rho_B(0) \right) \right],
\end{aligned} \quad (3.35)
$$

where S denotes system, B denotes bath (environment), and $\mathbf{1}_B$ is the identity operator in the bath Hilbert space. We also assume that the system+bath state factorizes at time $t = 0$ as $|\psi_0\rangle \otimes |0\rangle$, where ψ_0 is some pure system state. By using the cyclic property of the trace, we can rewrite this equation as

$$
\langle c(t) \rangle = \mathrm{tr}_S \left[c(0) \hat{\rho}_S(t) \right], \quad (3.36)
$$

where $\hat{\rho}_S(t)$ is the effective system density matrix

$$
\hat{\rho}_S(t) = \mathrm{tr}_B \left[U(t) \left(\rho_S(0) \otimes \rho_B(0) \right) U^\dagger(t) \right]. \quad (3.37)
$$

From Eq. (3.34) we get

$$
\begin{aligned}
\langle \mathrm{d}c(t) \rangle &= \langle 0, \psi_0 \left| \mathrm{d}c(t) \right| 0, \psi_0 \rangle \\
&= \left\langle \psi_0 \left| -i \left[c(t), H_{sys}(t) \right] + \mathcal{D}^\dagger[L(t)]c(t) \right| \psi_0 \right\rangle \mathrm{d}t \\
&= \mathrm{tr}_S \left[\left(-i \left[c(t), H_{sys}(t) \right] + \mathcal{D}^\dagger[L(t)]c(t) \right) \hat{\rho}_S(0) \right],
\end{aligned} \quad (3.38)
$$

But since we also have

$$
\langle \mathrm{d}c(t) \rangle = \mathrm{tr}_S \left[c(0) \mathrm{d}\hat{\rho}_S(t) \right], \quad (3.39)
$$

the cyclic property of the trace gives us an equation of motion for the effective density matrix,

$$
\mathrm{d}\hat{\rho}_S(t) = -i \left[H, \hat{\rho}_S(t) \right] \mathrm{d}t + \mathcal{D}[L] \hat{\rho}_S(t) \mathrm{d}t, \quad (3.40)
$$

where we have removed the time arguments $t = 0$ from the Schrödinger picture system operators. Remembering that $L = \sqrt{\kappa} a$, we see that we have rederived Eq. (3.4).

3.4 Photodetection

Let us apply the formalism above to a simple (in theory, not always in practice) measurement, photodetection. We return to our favorite example, a harmonic oscillator coupled to an environment. There are two measurement outcomes possible during a short time dt; either no photon is detected or one photon is detected. We calculate the corresponding Ω_i operators using the expression for the time evolution operator from Eq. (3.33):

$$
\begin{aligned}
\Omega_0(t+dt,t) &= \left\langle 0 \left| 1 - iH_{sys}dt + \sqrt{\kappa}\left(adB_t^\dagger - a^\dagger dB_t\right) - \frac{\kappa}{2}a^\dagger a dt \right| 0 \right\rangle \\
&= 1 - iH_{sys}dt - \frac{\kappa}{2}a^\dagger a dt, \tag{3.41}
\end{aligned}
$$

$$
\begin{aligned}
\Omega_1(t+dt,t) &= \left\langle 1 \left| 1 - iH_{sys}dt + \sqrt{\kappa}\left(adB_t^\dagger - a^\dagger dB_t\right) \right| 0 \right\rangle \\
&\quad + \left\langle 1 \left| \left(-iH_{sys}dt + \sqrt{\kappa}\left(adB_t^\dagger - a^\dagger dB_t\right)\right)^2 \right| 0 \right\rangle \\
&= \sqrt{\kappa}a\sqrt{dt}, \tag{3.42}
\end{aligned}
$$

where we have used the Itō rules for vacuum expectation values and $|1\rangle = \frac{1}{\sqrt{dt}}dB^\dagger(t)|0\rangle$ [16].

Inserting these results in Eq. (3.24) gives

$$
\begin{aligned}
\rho_0(t+dt) &= \frac{\left(1 - iH_{sys}dt - \frac{\kappa}{2}a^\dagger a dt\right)\rho_0(t)\left(1 + iH_{sys}dt - \frac{\kappa}{2}a^\dagger a dt\right)}{\left\langle\left(1 + iH_{sys}dt - \frac{\kappa}{2}a^\dagger a dt\right)\left(1 - iH_{sys}dt - \frac{\kappa}{2}a^\dagger a dt\right)\right\rangle} \\
&= \frac{\rho_0(t) - i\left[H_{sys},\rho_0(t)\right]dt - \frac{\kappa}{2}\left\{a^\dagger a,\rho_0(t)\right\}dt + \mathcal{O}(dt^2)}{1 - \kappa\left\langle a^\dagger a\right\rangle dt + \mathcal{O}(dt^2)} \\
&= \left(\rho_0(t) - i\left[H_{sys},\rho_0(t)\right]dt - \frac{\kappa}{2}\left\{a^\dagger a,\rho_0(t)\right\}dt\right) \\
&\quad \times \left(1 + \kappa\left\langle a^\dagger a\right\rangle dt\right) + \mathcal{O}(dt^2) \\
&= \rho_0(t) - i\left[H_{sys},\rho_0(t)\right]dt - \frac{\kappa}{2}\left\{a^\dagger a,\rho_0(t)\right\}dt \\
&\quad + \kappa\left\langle a^\dagger a\right\rangle\rho_0(t)dt + \mathcal{O}(dt^2), \tag{3.43}
\end{aligned}
$$

and carrying out a similar calculation for $\rho_1(t)$ leaves us with

$$
\begin{aligned}
d\rho_0 &= \left(-i\left[H_{sys},\rho_0(t)\right] + \kappa\left\langle a^\dagger a\right\rangle\rho_0 - \frac{\kappa}{2}\left\{a^\dagger a,\rho_0\right\}\right)dt, \tag{3.44} \\
d\rho_1 &= \frac{a\rho_1 a^\dagger}{\left\langle a^\dagger a\right\rangle} - \rho_1. \tag{3.45}
\end{aligned}
$$

Defining the stochastic process $N(t)$, which counts the number of photons detected up to time t, we get the stochastic increment $\mathrm{d}N(t)$. This increment has the properties $\mathrm{d}N(t)^2 = \mathrm{d}N(t)$, since in a small enough time interval one can only detect either 0 or 1 photons, and $\mathrm{E}\left[\mathrm{d}N(t)\right] = \kappa \left\langle a^\dagger a \right\rangle \mathrm{d}t$, which is the probability of detecting one photon during the time $\mathrm{d}t$. Using this notation we can write the stochastic master equation

$$
\begin{aligned}
\mathrm{d}\rho &= \left(-i\left[H_{sys}, \rho_0(t)\right] + \kappa \left\langle a^\dagger a \right\rangle \rho - \frac{\kappa}{2} \left\{ a^\dagger a, \rho \right\} \right) \mathrm{d}t \\
&+ \left(\frac{a\rho a^\dagger}{\langle a^\dagger a \rangle} - \rho \right) \mathrm{d}N(t),
\end{aligned}
\tag{3.46}
$$

which describes how the system state develops, conditioned on the measurement record $N(t)$. To make the connection with previous master equations, we remember that Eq. (3.46) describes a quantum trajectory. Averaging over many trajectories, using the expectation value for $\mathrm{d}N(t)$, lets us recover Eq. (3.4).

Also, the SME can be generalized to the case of an imperfect detector. Assuming that the detector only registers a fraction η (this parameter is known as the measurement efficiency) of the photons leaking out from the system, we recover an ordinary Lindblad term describing the loss of the undetected photons. The final expression for the SME is [16]

$$
\begin{aligned}
\mathrm{d}\rho &= \left(-\frac{i}{\hbar}\left[H, \rho\right] + (1-\eta)\kappa\mathcal{D}\left[a\right]\rho \right) \mathrm{d}t \\
&+ \mathcal{G}\left[a\right]\rho\,\mathrm{d}N(t) - \frac{1}{2}\eta\kappa\mathcal{M}\left[a^\dagger a\right]\rho\,\mathrm{d}t,
\end{aligned}
\tag{3.47}
$$

where we have introduced the notation $\mathcal{G}\left[c\right]\rho = \frac{c\rho c^\dagger}{\langle c^\dagger c \rangle} - \rho$, $\mathcal{M}\left[c\right]\rho = c\rho + \rho c^\dagger - \left\langle c + c^\dagger \right\rangle \rho$, and where now $\mathrm{E}\left[\mathrm{d}N(t)\right] = \eta\kappa \left\langle a^\dagger a \right\rangle \mathrm{d}t$. An SME of this type, with the addition of a qubit coupled to the harmonic oscillator, is central to Paper I.

3.5 Homodyne detection

As a good photodetector for microwave quantum optics has yet to be demonstrated, most experiments use a homodyne measurement instead. The theoretical model for a homodyne measurement is depicted in Fig. 3.2. The output from the system is fed into one of the two input ports of a 50/50
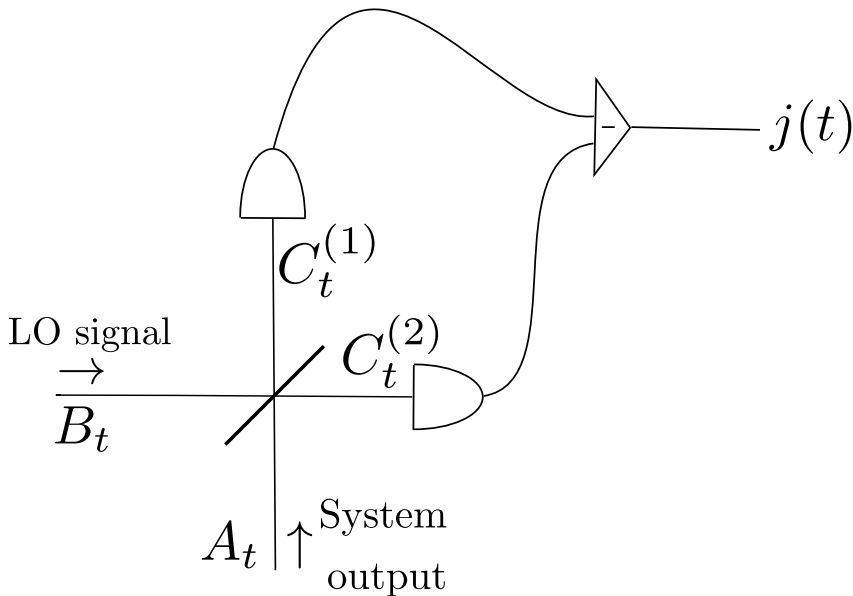
Figure 3.2: The model for homodyne detection.

beamsplitter. A strong coherent signal, from a local oscillator (LO), at the same frequency is applied to the other input port. The two outputs from the beamsplitter are then detected by separate photodetectors, and the final measurement signal, the *homodyne current*, is the difference of the two photocurrents. It should be clearly noted that this is a theoretical model; the actual experimental implementation is different (since there are no microwave photon detectors) [69].

We can use the same formalism as in the previous section to derive the Ω_i operators for each of the two photodetectors. However, we must remember that the inputs to the two detectors are mixes of the vacuum dB_t driven by the coherent signal, and the vacuum dA_t which is in contact with the system. For a 50/50 beamsplitter, these mixes are given by

$$dC_t^{(1)} = \frac{1}{\sqrt{2}}\left(dA_t + dB_t\right), \tag{3.48}$$

$$dC_t^{(2)} = \frac{1}{\sqrt{2}}\left(dA_t - dB_t\right). \tag{3.49}$$

We must also find the time evolution operator for the B vacuum. As this vacuum is driven by a coherent signal with amplitude β ($|\beta|^2$ is the

photon flux), we now get terms like $\beta^* dB_t$ instead of $\sqrt{\kappa} a^\dagger dB_t$ as we had previously. Keeping in mind that $|0\rangle$ now really means $|0\rangle_A \otimes |0\rangle_B$, we get

$$
\begin{aligned}
\Omega_0(t + dt, t) &= \left\langle 0 \left| 1 - iH_{sys}dt + \sqrt{\kappa} \left(a dA_t^\dagger - a^\dagger dA_t \right) + \beta dB_t^\dagger \right| 0 \right\rangle \\
&\quad + \left\langle 0 \left| -\beta^* dB_t - \frac{\kappa}{2} a^\dagger a dt - |\beta|^2 dt \right| 0 \right\rangle \\
&= 1 - iH_{sys}dt - \frac{\kappa}{2} \left(a^\dagger a + |\beta|^2 \right) dt, \quad\quad (3.50)
\end{aligned}
$$

$$
\Omega_{1/2}(t + dt, t) = \sqrt{\frac{\kappa}{2}} \left(a \pm \beta \right) \sqrt{dt}, \quad\quad (3.51)
$$

where we used $\langle 1|_{1/2} = \frac{1}{\sqrt{2}\sqrt{dt}} \langle 0| (dA_t + dB_t)$ and the Itō rules. With these results in hand, we can write down the equation of motion for the density matrix for the three different measurement results. Defining the stochastic photon counting processes $N_1(t)$ and $N_2(t)$ with corresponding stochastic increments, we get an SME.

The SME for homodyne detection is a result of taking the limit of an infinitely strong LO, *i.e.*, $\beta \to \infty$. Carrying through this analysis, which requires some work that is well described elsewhere [32, 60], eventually leads to the SME

$$
d\rho = -i[H, \rho] + \kappa \mathcal{D}[a]\rho + \sqrt{\kappa\eta}\mathcal{M}\left[a e^{-i\phi}\right]\rho dW(t), \quad\quad (3.52)
$$

where we have included the effect of measurement efficiency η, $dW(t)$ is a Wiener increment, and ϕ is a phase set by the local oscillator. The Wiener increment is a random variable with $E[dW(t)] = 0$ and variance dt. The phase ϕ determines which quadrature of the signal is measured. We see that averaging over many quantum trajectories given by Eq. (3.52) once again lets us recover Eq. (3.4).

The measurement signal is the homodyne current

$$
j(t)dt = \sqrt{\kappa\eta} \left\langle a e^{-i\phi} + a^\dagger e^{i\phi} \right\rangle dt + dW(t), \qu\quad (3.53)
$$

which one gets by taking the limit $\beta \to \infty$ of the normalized photocurrent $(N_1(t) - N_2(t))/\beta$ [32, 60]. Eq. (3.53) shows two things clearly. Firstly, changing ϕ indeed determines which quadrature is measured. Secondly, the signal will be noisy, even for a vacuum bath, due to the stochastic increment $dW(t)$.

The SME for homodyne detection is very important for the calculations in Paper I. With one or two qubits coupled dispersively to the resonator,

a homodyne measurement on the resonator output can give very different types of information about the qubit state(s) depending on which quadrature is measured.

Chapter 4

Cascaded Quantum Systems

In the previous chapter we developed tools to deal with input to, and output from, open quantum systems, and measurements on these signals. A natural extension of these considerations is to investigate what happens when we use the output from one system as the input for another system. In this chapter, we will introduce a convenient formalism, the (S, L, H) *formalism* [17, 18], that allows us to cascade quantum systems in a multitude of ways. Furthermore, we also look at a closely connected formalism that allows us to calculate what happens when Fock state photons are used as input to a system.

4.1   The (S,L,H) formalism

Let us assume we have two systems, described by Hamiltonians H_1 and H_2, respectively. Assume furthermore that the first system is coupled via an input-output port to the environment by a coupling operator L_1, and that the output from the first system is fed into the second system, which is coupled to that output by L_2. Finally, we assume that there is no time delay in relaying a signal from the first system to the second. The time evolution operator for the combined system can then be found by first time evolving the state of system 1 for a small time $\mathrm{d}t$, then evolving the state of system 2 for that small time, and so on. The first part of this time

evolution is then, using Eq. (3.33), given by

$$
\begin{aligned}
U_{\mathrm{d}t}^{(2)} U_{\mathrm{d}t}^{(1)} &= \left(1 + \mathrm{d}U_0^{(2)}\right)\left(1 + \mathrm{d}U_0^{(1)}\right) = 1 - i\left(H_1 + H_2\right)\mathrm{d}t \\
&\quad + \left(L_1 + L_2\right)\mathrm{d}B_0^\dagger - \left(L_1^\dagger + L_2^\dagger\right)\mathrm{d}B_0 \\
&\quad - \frac{1}{2}\left(L_1^\dagger L_1 + L_2^\dagger L_2\right)\mathrm{d}t - L_2^\dagger L_1 \mathrm{d}t \\
&= 1 - i\left(H_1 + H_2 + \frac{1}{2i}\left(L_2^\dagger L_1 - L_1^\dagger L_2\right)\right)\mathrm{d}t \\
&\quad - \frac{1}{2}\left(L_1 + L_2\right)^\dagger\left(L_1 + L_2\right)\mathrm{d}t \\
&\quad + \left(L_1 + L_2\right)\mathrm{d}B_0^\dagger - \left(L_1 + L_2\right)^\dagger \mathrm{d}B_0. \quad (4.1)
\end{aligned}
$$

From this, we see that the total system behaves as if it had a Hamiltonian $H = H_1 + H_2 + \frac{1}{2i}\left(L_2^\dagger L_1 - L_1^\dagger L_2\right)$, and coupled to the environment via an operator $L = L_1 + L_2$ [68].

The above derivation suggests that an open quantum system could be assigned a doublet $G = (L,H)$, and that the *series product* of two systems is given by

$$
G = G_2 \triangleleft G_1 = \left(L_1 + L_2, H_1 + H_2 + \frac{1}{2i}\left[L_2^\dagger L_1 - L_1^\dagger L_2\right]\right). \quad (4.2)
$$

We note that the total doublet is not invariant under interchange of 1 and 2. This reflects the ordering of the two systems; the output from one is fed into the other, not the other way around. This formalism can be extended to systems having several input-ouput ports. The L then becomes a column vector of coupling operators, and the above expression still holds.

So far, we have only used the L and H in (S,L,H). So, what is the S? The S is called the scattering matrix. It is an addition to the formalism needed to describe systems with scattering between multiple channels [18]. The typical example is a beamsplitter. A beamsplitter has neither L nor H, it is simply a device that takes two inputs and mixes them into two outputs. The S describes this scattering process, and provides a way to use the (S,L,H) formalism to handle connections between a multitude of different quantum systems. To exemplify, the triplet for a 50/50 beamsplitter is given by

$$
G_{BS} = \left(\begin{pmatrix} \frac{1}{\sqrt{2}} & -\frac{1}{\sqrt{2}} \\ \frac{1}{\sqrt{2}} & \frac{1}{\sqrt{2}} \end{pmatrix}, \begin{pmatrix} 0 \\ 0 \end{pmatrix}, 0\right). \quad (4.3)
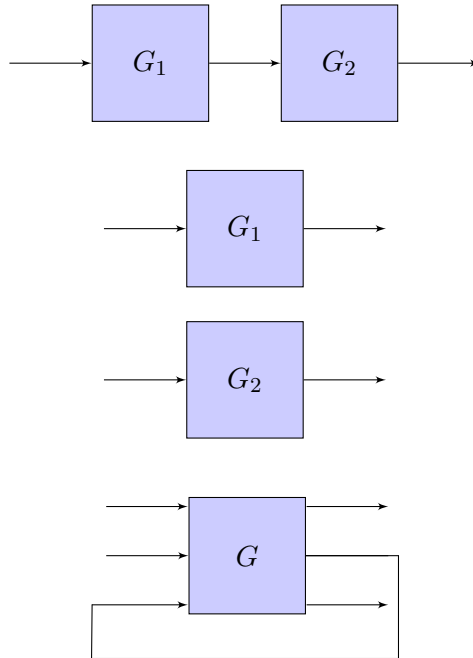$$

Figure 4.1: The three operations that the (S,L,H) formalism can handle. From top to bottom: series product $G_2 \triangleleft G_1$, concatenation product $G_1 \boxplus G_2$, and feedback.

Actually, the S also comes in handy for a single-channel case. In a situation when the distance between two systems, G_1 and G_2, is non-negligible, the (S,L,H) formalism can still work if one inserts a phase shift between the two systems in the calculation. This is done by placing the triplet $G_\phi = (e^{i\phi},0,0)$ between G_1 and G_2.

Another component one would like to incorporate in many setups is a coherent signal. Noting that this is just a displaced vacuum, one can show that a coherent signal, sending in $|\alpha|^2$ photons per second, is described by the triplet $G_\alpha = (1,\alpha,0)$.

In the subsection below we list the three complete rules for (S,L,H) calculations, including the modification to the series product derived above brought about by the inclusion of S.

4.1.1 (S,L,H) rules

Here, we summarize the calculation rules used in the (S,L,H) formalism. The three operations are illustrated in Fig. 4.1. The series product $\triangleleft$ generalizes, when including the scattering matrix, to [17, 18]

$$
G_2 \triangleleft G_1 = \left(S_2 S_1, S_2 L_1 + L_2, H_1 + H_2 + \frac{1}{2i} \left(L_2^\dagger S_2 L_1 - L_1^\dagger S_2^\dagger L_2 \right) \right). \quad (4.4)
$$

To assemble systems we also need the *concatenation product* $\boxplus$ (stacking channels), which is given by

$$
G_2 \boxplus G_1 = \left(\begin{pmatrix} S_2 & 0 \\ 0 & S_1 \end{pmatrix}, \begin{pmatrix} L_2 \\ L_1 \end{pmatrix}, H_2 + H_1 \right). \quad (4.5)
$$

Finally, there is also a rule for the feedback operation $[(S,L,H)]_{k \to l} = (\tilde{S}, \tilde{L}, \tilde{H})$, which represents feeding the kth output of a system into the lth input of the same system. The result is

$$
\tilde{S} = S_{[k/l]} + \begin{pmatrix} S_{1,l} \\ \vdots \\ S_{k-1,l} \\ S_{k+1,l} \\ \vdots \\ S_{n,l} \end{pmatrix} (1 - S_{k,l})^{-1} \left(S_{k,l} \ \ldots \ S_{k,l-1} \ S_{k,l+1} \ \ldots \ S_{k,n} \right),
$$

$$
\tilde{L} = L_{[k]} + \begin{pmatrix} S_{1,l} \\ \vdots \\ S_{k-1,l} \\ S_{k+1,l} \\ \vdots \\ S_{n,l} \end{pmatrix} (1 - S_{k,l})^{-1} L_k,
$$

$$
\tilde{H} = H + \frac{1}{2i} \left(\left(\sum_{j=1}^{n} L_j^\dagger S_{j,l} \right) (1 - S_{k,l})^{-1} L_k - \text{h.c.} \right), \quad (4.6)
$$

where $S_{[k/l]}$ and $L_{[k]}$ are the original scattering matrix and coupling vector with row k and column l removed [70].

Once we have the (S,L,H) for our total system,

$$G = \left(S, \begin{pmatrix} L_1 \\ \vdots \\ L_n \end{pmatrix}, H\right), \tag{4.7}$$

we can extract the master equation for the total system as

$$\dot{\rho} = -i\left[H, \rho\right] + \sum_{i=1}^{n} \mathcal{D}\left[L_i\right]\rho. \tag{4.8}$$

The average output from port i of the system is simply given by $\langle L_i \rangle$.

4.1.2 An (S,L,H) example - coupled cavities

Let us look at an example of how to use the (S,L,H) formalism. We choose as our system a simplified version of a setup used in Paper I to model a bandpass filter. Imagine a coherent signal impinging on a two-sided cavity from the left. The output from the right side of the cavity is then sent on, hitting a second two-sided cavity from the left. We imagine there being a circulator between the two cavities so that the signal reflected from the second cavity doesn't return to the first cavity. The setup is depicted in Fig. 4.2.

We begin by writing down the (S,L,H) triplets of the different system components. The incoming coherent signal is simply given by

$$G_\beta = (1, \beta, 0), \tag{4.9}$$

where $|\beta|^2$ is the photon flux, measured in units of photons per second. The first cavity has the triplet

$$\begin{aligned} G_a &= \left(\begin{pmatrix} 1 & 0 \\ 0 & 1 \end{pmatrix}, \begin{pmatrix} \sqrt{\kappa_1}a \\ \sqrt{\kappa_2}a \end{pmatrix}, H_a\right) \\ &= (1, \sqrt{\kappa_1}a, H_a) \boxplus (1, \sqrt{\kappa_2}a, 0) \equiv G_{a1} \boxplus G_{a2} \end{aligned} \tag{4.10}$$

where a is the annihilation operator for the mode in the cavity, κ_1 and κ_2 are the photon loss rates through the left and the right side of the cavity, respectively, and

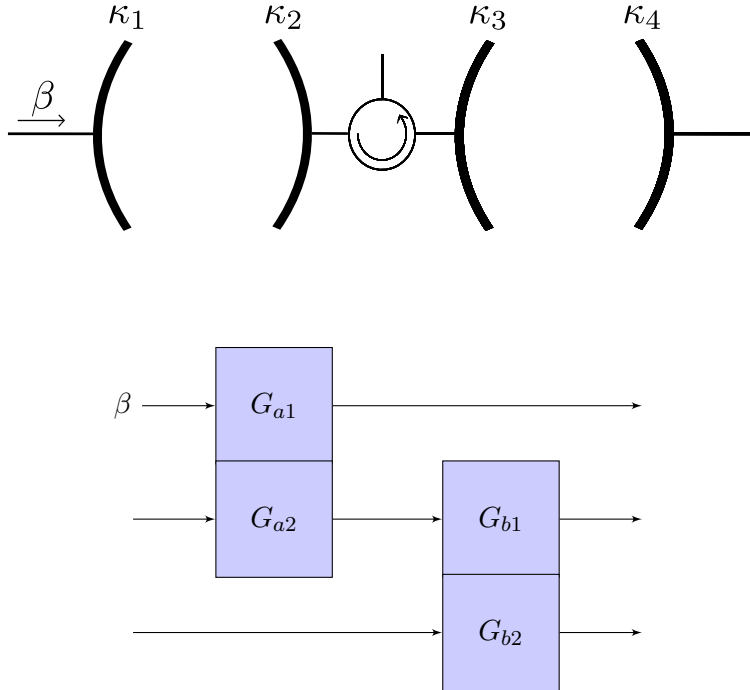$$H_a = \Delta_a a^\dagger a \tag{4.11}$$

Figure 4.2: Top: Illustration of the setup for the two coupled cavities. Bottom: A schematic picture of the same setup, showing how to set up the (S,L,H) triplet for the total system. It should be understood as follows: The uppermost input is that which is fed in through the left side of the first cavity, the middle input is that which enters the first cavity from the right, and the last input is that which enters the second cavity from the right. The first output is that which exits, or is reflected from, the left side of the first cavity. The second output is that which exits, or is reflected from, the left side of the second cavity. Finally, the last output exits, or is reflected from, the right side of the second cavity.

is the Hamiltonian of the cavity in a frame rotating with the frequency ω_β of the input signal. $\Delta_a = \omega_a - \omega_\beta$ is the detuning from the cavity frequency ω_a. It is useful to decompose the cavity triplet like this to properly deal with using one of its outputs as the input for the second cavity, which has the triplet

$$G_b = G_{b1} \boxplus G_{b2} = (1, \sqrt{\kappa_3}b, H_b) \boxplus (1, \sqrt{\kappa_4}b, 0), \tag{4.12}$$

with everything defined in analogy with the case of the first cavity.

We can now, using the schematic in Fig. 4.2, calculate the triplet for the combined system,

$$
\begin{aligned}
G &= (I \boxplus G_{b1} \boxplus G_{b2}) \lhd ((G_{a1} \lhd G_\beta) \boxplus G_{a2} \boxplus I) \\
&= \left(\mathbf{1}_3, \begin{pmatrix} 0 \\ \sqrt{\kappa_3}b \\ \sqrt{\kappa_4}b \end{pmatrix}, H_b \right) \\
&\quad \lhd \left(\mathbf{1}_3, \begin{pmatrix} \beta + \sqrt{\kappa_1}a \\ \sqrt{\kappa_2}a \\ 0 \end{pmatrix}, H_a + \frac{1}{2i}\sqrt{\kappa_1}\left(\beta a^\dagger - \beta^* a \right) \right) \\
&= \left(\mathbf{1}_3, \begin{pmatrix} \beta + \sqrt{\kappa_1}a \\ \sqrt{\kappa_2}a + \sqrt{\kappa_3}b \\ \sqrt{\kappa_4}b \end{pmatrix}, \right. \\
&\qquad \left. H_a + H_b + \frac{1}{2i}\sqrt{\kappa_1}\left[\beta a^\dagger - \beta^* a \right] + \frac{1}{2i}\sqrt{\kappa_2 \kappa_3}\left[ab^\dagger - a^\dagger b \right] \right) \tag{4.13}
\end{aligned}
$$

where the inserted identity triplets $I = (1,0,0)$ make sure that the right channels are connected, and $\mathbf{1}_n$ denotes the $n \times n$ identity matrix.

From Eq. (4.8) we now see that the master equation for the total system is

$$
\begin{aligned}
\dot{\rho} &= -i\left[H_a + H_b + \frac{1}{2i}\sqrt{\kappa_1}\left(\beta a^\dagger - \beta^* a \right) + \frac{1}{2i}\sqrt{\kappa_2 \kappa_3}\left(ab^\dagger - a^\dagger b \right), \rho \right] \\
&\quad + \mathcal{D}\left[\beta + \sqrt{\kappa_1}a \right]\rho + \mathcal{D}\left[\sqrt{\kappa_2}a + \sqrt{\kappa_3}b \right]\rho + \mathcal{D}\left[\sqrt{\kappa_4}b \right]\rho. \tag{4.14}
\end{aligned}
$$

Noting that

$$
\begin{aligned}
\mathcal{D}\left[a + b \right]\rho &= \mathcal{D}\left[a \right]\rho + \mathcal{D}\left[b \right]\rho + a\rho b^\dagger + b\rho a^\dagger \\
&\quad - \frac{1}{2}\left(\left(a^\dagger b + b^\dagger a \right)\rho + \rho\left(a^\dagger b + b^\dagger a \right) \right), \tag{4.15}
\end{aligned}
$$

after some algebra we are able to rewrite the master equation as

$$
\begin{aligned}
\dot{\rho} \;=\; & -i\left[H_a + H_b - i\sqrt{\kappa_1}\left(\beta a^\dagger - \beta^* a\right), \rho\right] \\
& + (\kappa_1 + \kappa_2)\,\mathcal{D}\left[a\right]\rho + (\kappa_3 + \kappa_4)\,\mathcal{D}\left[b\right]\rho \\
& + \sqrt{\kappa_2 \kappa_3}\left(\left[b, \rho a^\dagger\right] + \left[a\rho, b^\dagger\right]\right).
\end{aligned}
\tag{4.16}
$$

To see what signal comes out from the right side of the second cavity we would solve this master equation and look at $\sqrt{\kappa_4}\,\langle b\rangle$.

   To prove that a cavity acts as a filter for a signal, it is enough to study the steady state of the signal that is reflected from the first cavity, *i.e.*, $\beta + \sqrt{\kappa_1}\,\langle a\rangle_{ss}$ (as given by the input-ouput relation Eq. (3.16)). Using commutation relations for the a's and b's, and the cyclic property of the trace, we get that the steady state of $\langle a\rangle$ is given by

$$
0 = \frac{\mathrm{d}}{\mathrm{d}t}\langle a\rangle = \mathrm{tr}\,(a\dot{\rho}) = -\sqrt{\kappa_1}\beta - \left(i\Delta_a + \frac{1}{2}\kappa_1 + \frac{1}{2}\kappa_2\right)\langle a\rangle, \tag{4.17}
$$

which leads us to

$$
\langle a\rangle_{ss} = -\frac{\sqrt{\kappa_1}\beta}{i\Delta_a + \frac{1}{2}\kappa_1 + \frac{1}{2}\kappa_2}. \tag{4.18}
$$

Assuming $\kappa_1 = \kappa_2 \equiv \kappa_a$, the steady-state reflected signal form the first cavity is thus

$$
\beta - \frac{\kappa_a \beta}{i\Delta_a + \kappa_a}. \tag{4.19}
$$

We see that the photon flux, the absolute value squared of the above quantity, is 0 when the input signal is on resonance with the cavity, *i.e.*, when $\Delta_a = 0$. Furthermore, the photon flux is exactly half of the input when $\Delta_a = \pm\kappa_a$. This clearly shows that the cavity acts as a filter with bandwidth $2\kappa_a$.

4.2   A formalism for Fock-state input

The (S,L,H) formalism is indeed versatile, but there are some situations where additional efforts are needed. One example is the problem of Fock state photons impinging on a quantum system. To treat this problem properly, a formalism including a description of the photon wavepacket

is needed. Such a formalism, which is derived using the by now familiar quantum stochastic calculus, was recently presented [19], drawing on theoretical efforts of the last decades [71, 72].

First, we define the Fock state [73]

$$|1_\xi\rangle = \int_{-\infty}^{\infty} d\omega \tilde{\xi}(\omega) b^\dagger(\omega)|0\rangle, \tag{4.20}$$

where $\tilde{\xi}(\omega)$ is the *spectral density function* describing how the photon is superposed over different modes. The spectrum is assumed to be confined to a small bandwidth around a center frequency ω_c, which is close to the relevant frequency of the system to be interacted with. We then define a slowly varying envelope $\tilde{\xi}(\omega) \to \tilde{\xi}(\omega)e^{-i\omega_c t}$. The Fourier transform $\mathcal{F}[\tilde{\xi}(\omega)] = \xi(t)$ is the temporal shape of the photon, normalized according to $\int dt |\xi(t)|^2 = 1$. In the time domain we then have

$$|1_\xi\rangle = \int_{-\infty}^{\infty} dt \xi(t) b_{in}^\dagger(t)|0\rangle, \tag{4.21}$$

and a Fock state with N photons can be defined as

$$|N_\xi\rangle = \frac{1}{\sqrt{N!}} \left(\int_{-\infty}^{\infty} dt \xi(t) b_{in}^\dagger(t) \right)^N |0\rangle. \tag{4.22}$$

Assuming that the system+bath state factorizes at time $t = 0$ as $|\psi\rangle \otimes |N_\xi\rangle$, where ψ is some pure system state, we now proceed like in Section 3.3 to derive an equation for the effective density matrix of the system. It turns out to be more complicated than before, since the system now can absorb excitations from the bath, which was not the case when the bath was in the vacuum state. Remember that all equations in Section 3.3 were derived using the Itō vacuum expectation rules for combinations of dB_t and $dB_t^\dagger$. Fortunately, it can be shown that these rules still hold unchanged even for asymmetric expectation values $\langle M_\xi |...| N_\xi\rangle$ [19]. Thus, Eq. (3.33) and Eq. (3.34) can still be used.

Using the identity

$$dB_t|N_\xi\rangle = dt\sqrt{N}\xi(t)|N - 1_\xi\rangle, \tag{4.23}$$

which can be shown rather easily [19], together with Eq. (3.34) gives that the equation of motion for the expectation value of a system operator c in

the Heisenberg picture is

$$
\begin{aligned}
\langle \mathrm{d}c(t) \rangle &= \langle N_\xi, \psi \,|\mathrm{d}c(t)|\, N_\xi, \psi \rangle \\
&= \Big\langle N_\xi, \psi \,\Big|\, -i\,[c(t), H_{sys}(t)] + \mathcal{D}^\dagger[L(t)]c(t) \,\Big|\, N_\xi, \psi \Big\rangle \,\mathrm{d}t \\
&\quad + \Big\langle N_\xi, \psi \,\Big|\, [c(t), L(t)]\,\mathrm{d}B_t^\dagger + \Big[L^\dagger(t), c(t)\Big]\,\mathrm{d}B_t \,\Big|\, N_\xi, \psi \Big\rangle \\
&= \Big\langle N_\xi, \psi \,\Big|\, -i\,[c(t), H_{sys}(t)] + \mathcal{D}^\dagger[L(t)]c(t) \,\Big|\, N_\xi, \psi \Big\rangle \,\mathrm{d}t \\
&\quad + \langle N - 1_\xi, \psi \,|[c(t), L(t)]|\, N_\xi, \psi \rangle\, \xi^*(t)\mathrm{d}t \\
&\quad + \Big\langle N_\xi, \psi \,\Big|\, \Big[L^\dagger(t), c(t)\Big] \,\Big|\, N - 1_\xi, \psi \Big\rangle\, \xi(t)\mathrm{d}t. \qquad (4.24)
\end{aligned}
$$

Apparently, we need to evaluate several expectation values on the form $\langle n_\xi, \psi \,|X(t)|\, m_\xi, \psi \rangle$ for different system operators $X(t)$ in order to eventually find $\langle c(t) \rangle$. From Eq. (3.34) and Eq. (4.23) we get

$$
\begin{aligned}
\langle n_\xi, \psi \,|\mathrm{d}X(t)|\, m_\xi, \psi \rangle &= \langle n_\xi, \psi \,|-i\,[X(t), H_{sys}(t)]|\, m_\xi, \psi \rangle\,\mathrm{d}t \\
&\quad + \Big\langle n_\xi, \psi \,\Big|\, \mathcal{D}^\dagger[L(t)]X(t) \,\Big|\, m_\xi, \psi \Big\rangle\,\mathrm{d}t \\
&\quad + \Big\langle n_\xi, \psi \,\Big|\, \Big[L^\dagger(t), X(t)\Big] \,\Big|\, m - 1_\xi, \psi \Big\rangle\, \sqrt{m}\,\xi(t)\mathrm{d}t \\
&\quad + \langle n - 1_\xi, \psi \,|[X(t), L(t)]|\, m_\xi, \psi \rangle\, \sqrt{n}\,\xi^*(t)\mathrm{d}t. \quad (4.25)
\end{aligned}
$$

Thus, we see that we end up with a system of equations that couple downwards, and solving them starting with $\langle 0, \psi \,|X(t)|\, 0, \psi \rangle$ will eventually give $\langle c(t) \rangle$. The initial conditions are

$$
\langle n_\xi, \psi \,|X(0)|\, m_\xi, \psi \rangle = \left\{ \begin{array}{ll} \langle \psi \,|X(0)|\, \psi \rangle, & \text{if } n = m, \\ 0, & \text{if } n \neq m. \end{array} \right. \qquad (4.26)
$$

To get a description in terms of an effective system density matrix instead, we define $\rho_{m,n}$ in analogy with Eq. (3.36),

$$
\langle n_\xi, \psi \,|X(t)|\, m_\xi, \psi \rangle = \mathrm{tr}_S\left(\rho_{m,n}(t)X\right). \qquad (4.27)
$$

With this definition Eq. (4.25) can either be written as

$$
\begin{aligned}
\langle n_\xi, \psi \,|\mathrm{d}X(t)|\, m_\xi, \psi \rangle &= \mathrm{tr}_S\left(\rho_{m,n}(t)\left(-i\,[X, H_{sys}] + \mathcal{D}^\dagger[L]X\right)\right)\mathrm{d}t \\
&\quad + \mathrm{tr}_S\left(\rho_{m,n-1}(t)\,[X, L]\right)\sqrt{n}\,\xi^*(t)\mathrm{d}t \\
&\quad + \mathrm{tr}_S\left(\rho_{m-1,n}(t)\,\Big[L^\dagger, X\Big]\right)\sqrt{m}\,\xi(t)\mathrm{d}t, \qquad (4.28)
\end{aligned}
$$

or as

$$\langle n_\xi, \psi \left| \mathrm{d}X(t) \right| m_\xi, \psi \rangle \;\; = \;\; \mathrm{tr}_S \left(\mathrm{d}\rho_{m,n}(t)X \right) \mathrm{d}t. \qquad (4.29)$$

Using these two equations together with the cyclic property of the trace gives the system of equations

$$\begin{aligned}
\frac{\mathrm{d}\rho_{m,n}(t)}{\mathrm{d}t} \;\; = \;\; & -i\left[H, \rho_{m,n}(t)\right] + \mathcal{D}\left[L\right]\rho_{m,n}(t) \\
& + \sqrt{n}\left[L, \rho_{m,n-1}(t)\right]\xi^*(t) \\
& + \sqrt{m}\left[\rho_{m-1,n}(t), L^\dagger\right]\xi(t),
\end{aligned} \qquad (4.30)$$

which can be solved by starting from the equation for $\rho_{0,0}(t)$, and working your way upwards. From Eq. (4.26) and Eq. (4.27) it follows that the initial conditions are

$$\rho_{m,n}(0) = \left\{ \begin{array}{ll} |\psi\rangle\langle\psi|, & \text{if } n = m, \\ 0, & \text{if } n \neq m. \end{array} \right. \qquad (4.31)$$

Note that $\rho_{m,n} = \rho_{n,m}^\dagger$, which reduces the number of equations needed to be solved. The final result is $\rho_{N,N}(t)$, which allows us to calculate the expectation value of any system operator when a wavepacket containing N photons interacts with the system.

This formalism can be extended in a number of ways. For example, it allows for the bath state to be a superposition of Fock states. Also, one can include a coupling between the system and the number noise increment $\mathrm{d}\Lambda(t) = b_{in}^\dagger(t)b_{in}(t)\mathrm{d}t$, but these things are outside the scope of this thesis as they are not used in Paper II. The interested reader is referred to Ref. [19].

4.2.1 Example - a photon and an atom

We illustrate the formalism for Fock state input using the simplest example possible: a single-photon wavepacket impinging on a two-level atom. The atom has the Hamiltonian, in the rotating frame of the photon center frequency ω_{ph},

$$H = \frac{\Delta}{2}\sigma_z, \qquad (4.32)$$

where $\Delta = \omega_0 - \omega_{ph}$, and ω_0 is the transition frequency of the atom. We assume the photon wavepacket to have the Gaussian envelope

$$\xi(t) = \left(\frac{\Gamma^2}{2\pi}\right)^{1/4} \exp\left(-\frac{\Gamma^2(t - t_{ph})^2}{4}\right), \qquad (4.33)$$
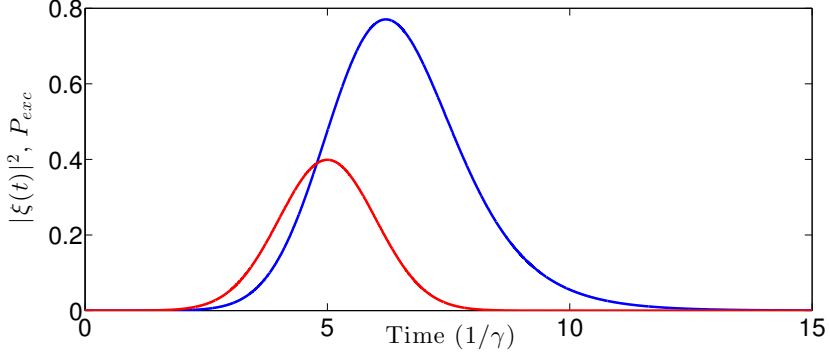
Figure 4.3: The dynamics of a single-photon wavepacket encountering a two-level atom. The red line shows the temporal shape of the Gaussian wavepacket of the photon, and the blue line shows the excitation probability of the atom as a function of time. Parameters: $\Delta = 0$, $t_{ph} = 5/\gamma$, $\Gamma = \gamma$, $\rho_{sys}(0) = |0\rangle\langle 0|$.

where t_{ph} is the time when the center of the photon wavepacket arrives at the atom, and Γ is the bandwidth of the photon.

The coupled density matrix equations become

$$\dot{\rho}_{0,0} = -i\left[\frac{\Delta}{2}\sigma_z, \rho_{0,0}\right] + \gamma \mathcal{D}\left[\sigma_-\right]\rho_{0,0}, \tag{4.34}$$

$$\dot{\rho}_{0,1} = -i\left[\frac{\Delta}{2}\sigma_z, \rho_{0,1}\right] + \gamma \mathcal{D}\left[\sigma_-\right]\rho_{0,1} + \xi^*(t)\left[\sqrt{\gamma}\sigma_-, \rho_{0,0}\right], \tag{4.35}$$

$$\rho_{1,0} = \rho_{0,1}^\dagger, \tag{4.36}$$

$$\dot{\rho}_{1,1} = -i\left[\frac{\Delta}{2}\sigma_z, \rho_{1,1}\right] + \gamma \mathcal{D}\left[\sigma_-\right]\rho_{1,1} + \xi(t)\left[\rho_{0,1}, \sqrt{\gamma}\sigma_+\right]$$
$$+\xi^*(t)\left[\sqrt{\gamma}\sigma_-, \rho_{1,0}\right], \tag{4.37}$$

with initial conditions $\rho_{0,0}(0) = \rho_{1,1}(0) = \rho_{sys}(0)$, and $\rho_{0,1}(0) = \rho_{1,0}(0) = 0$.

The density matrix can be solved analytically by writing $\rho_{n,m}$ as a combination of Pauli matrices [74]. However, as this is somewhat tedious, we limit ourselves to plotting, in Fig. 4.3, numerical solutions for the atom excitation probability $P_{exc}(t)$. This shows how the arrival of the photon leads to a high probability of exciting the atom when the photon is on resonance. The exact probability depends on the wavepacket shape [75].

In paper II, we perform a similar calculation to model the effect of a single photon arriving at a three-level transmon. The photon is close to

the resonance frequency of the first transition of the transmon. We study, for different shapes of the photon wavepacket, how the presence of the photon affects a coherent probe which is close to the second transition of the transmon. Even in this case one can get far by a purely analytical treatment.

Chapter 5

Paper Overview

Here we give an overview of the two papers on which this thesis is based. We explain the main ideas of the papers, and show how the theoretical methods of the previous chapters are applied. The main theme in both papers is measurements on a quantum system, which means that the use of SMEs are central to achieve results. Also, in both papers we cascade quantum systems, using the techniques of Chapter 4.

5.1 Paper I - Undoing measurement-induced dephasing in circuit QED

As was discussed in Chapter 1, parity measurements on qubits are an integral part of many error correction schemes for quantum computing. In 2010 Lalumierè *et al.* [15] described how a parity measurement in circuit QED can be carried out in practice. The idea is to place two qubits in a cavity, tune the system into the dispersive regime, and send in a coherent microwave signal at the resonance frequency of the cavity. For suitable parameters a homodyne detection in one quadrature of the outgoing signal will then only reveal information about the parity of the two qubits, and no information about their individual states. However, akin to the example in Section 3.2, the parity measurement gives phase kicks to the states in one of the parity subspaces. Averaging over many measurements, this looks like measurement-induced dephasing, which the authors show using the formalism of stochastic master equations.

In Ref. [76] Tornberg and Johansson showed that part of this dephasing can be undone. It turns out that monitoring the homodyne current (the

measurement signal) gives information about the phase kicks, similar to the example in Section 3.2. However, it appeared that only part of the information about the phase kicks could be extracted this way, and the problem of measurement-induced dephasing remained.

In Paper I, we look at measurements on both one and two qubits, and both homodyne detection and photodetection. We show that all the information about phase kicks can be extracted from the measurement signal, and thus that the measurement-induced dephasing in principle can be completely undone.

The key insight was that Ref. [76] considered the steady state case, *i.e.*, the coherent probe is turned on at time $t = 0$ and we try to undo the phase kicks we have information about once a long time has passed. The problem with this approach is that there will always be probe photons left in the cavity which have yet to leak out and reach the detector. Each such probe photon is entangled with the qubits and carries information about their phase. The solution is simple: we analyze the situation where the probe signal has been turned off at a time $t = t_{\text{off}} > 0$ and we have waited some time after that to let the remaining photons leak out of the cavity.

In this way we acquire all information about the phase kicks. For the case of homodyne detection the homodyne current from time $t = 0$ is needed, while for the case of photodetection one has to keep track of all the times when a photon has been detected. The calculation for the case of photodetection, including tracing out the cavity degrees of freedom to derive an effective SME for one qubit, is not done previously to our knowledge. The effective SME for homodyne detection has been derived previously [15, 77], but the result that the probe signal can be turned off to undo all the measurement-induced dephasing is new.

The positive result on undoing the phase kicks is of course only achieved in the limit of perfect detectors. Presently, there is still a lack of photodetectors for microwave quantum optics, and the homodyne detection schemes still suffer from problems with amplifier noise. To see if our results could be tested with currently available experimental equipment we modelled the case of homodyne detection with imperfect detectors and limited bandwidth. We used the (S,L,H) formalism to insert a second cavity (acting as a bandpass filter) through which the output from the cavity with the qubits was passed.

This model shows that undoing some of the measurement-induced dephasing could be undone already with existing technology. As amplifiers

are steadily improving towards being quantum-limited, this kind of quantum feedback experiment might soon be realized.

5.2   Paper II - Breakdown of the cross-Kerr scheme for photon counting

In Chapter 1, we briefly discussed the drawbacks of doing microwave quantum optics with superconducting circuits. One example was the lack of a good photodetector (though there are some suggestions trying to remedy this [78, 79, 80]). In Paper II, we investigate the possibility of using a three-level transmon to mediate a cross-Kerr type interaction between photons. A Kerr interaction between two modes, with operators a and b, has the form $\chi a^\dagger a b^\dagger b$. Thus, the presence of photons in one mode will change the frequency of the photons in the other mode, giving them a phase shift.

In our approach, a single photon, which we wish to detect, is close to resonance with the first transition in the transmon. The idea is that the arrival of this photon will induce a phase shift of a coherent signal, which is close to resonance with the second transition of the transmon. We need to find out whether this shift is big enough to give a signal that is discernible from noise.

We model the system at hand in two different ways. In the first approach we place a cavity to the left of the transmon, and initialize with one photon inside. Using the (S,L,H) formalism we can derive the master equation for the total system. Then, adding a homodyne measurement on the coherent probe after the transmon gives us a stochastic master equation. By numerically simulating many quantum trajectories, some with one photon in the cavity and some with zero photons in the cavity, we get a distribution of measurement results (integrated homodyne currents) for each case. From the separation and widths of the two distributions we extract the *signal-to-noise ratio* (SNR).

The second approach is to use the Fock-state input formalism of the previous chapter. This is advantageous, as it allows us to consider different shapes of photon wavepackets (the photon leaking out from a cavity can only have one shape). Furthermore, it turns out that the system of equations for the density matrix is analytically solvable. We are thus able to extract the SNR in a different way than before, and it yields the same results as the first approach.

That being said, the results are somewhat disheartening for experi-

mentalists waiting patiently for a microwave photodetector. We find no parameter regime where the SNR exceeds 1 (which is necessary to make a good detector). Even putting several transmons after each other in the transmission line does not help, as they collectively act as one single transmon if they are too close, and if they are far apart they still fail to give any useful amplification, as a large impact on the probe is tied to the signal photon being reflected (which means it will not interact with the rest of the transmons).

Other ideas, such as squeezing the probe field and varying the ratio of the two transmon relaxation rates, also fail to produce a good SNR. There appears to be a fundamental limit here which hinders us from achieving photon detection in this setup.

Chapter 6

Summary and outlook

In this thesis, we investigated two types of measurements in quantum optics. To describe the effects of weak measurements on quantum systems, we used quantum stochastic calculus, which we introduced in Chapter 3. Furthermore, we also used formalisms for cascading quantum systems, which is described in Chapter 4. We mainly envision our results being used in the field of microwave quantum optics with superconducting circuits, the basic elements of which were introduced in Chapter 2.

In Paper I, we showed how unwanted measurement back-action (in the form of measurement-induced dephasing) could be undone for certain measurements on one and two qubits dispersively coupled to a resonator. The results were shown to hold for both homodyne detection and photodetection. Basically, the photons coming out of the resonator are entangled with the qubit(s), and measuring them will either give information about the qubit state(s), which gives a projection, or about the measurement-induced phase kick, which can be undone. The most important application of this result will probably be improved parity measurements, which are needed to implement error-correcting surface codes for quantum computing. As a first step, it could also be used for an interesting quantum feedback experiment.

In Paper II, we discussed the possibility of using a three-level transmon to mediate a cross-Kerr type interaction between photons. The hope was to use this as a photon detector in the microwave regime, the lack of which is an annoying gap in the microwave quantum optics toolbox. However, it turned out that there are fundamental limitations to this setup, resulting in a signal-to-noise ratio below 1. Even some modifications to the original

idea, such as cascading several transmons in a row, or using a squeezed probe field, unfortunately turn out to be dead ends.

Looking to the future, we note that there now exists a good theoretical toolbox that can handle complex interconnection of quantum systems, and measurements on the output of these systems. There is also software available to help with many of these calculations [70, 81]. Considering this, and the fact that experimental results for setups with one or a few qubits show ever better coherence times and very good control capabilities, it seems that we are ready to investigate more advanced setups. There has of course already been some work done on quantum feedback [65, 82, 83] and possible setups with many interconnected quantum systems [84, 85, 86], but the possibilities are vast and beckoning for attention. For instance, we have not given up on the ideas for photodetection from Paper II. We are currently investigating the possibility of cascading several transmons with circulators in between. This would break time-reversal symmetry, and seems to provide a loophole to escape the limitations we saw in Paper II.

Bibliography

[1] C. R. Monroe, D. M. Meekhof, B. E. King, and D. J. Wineland. A "Schrödinger Cat" Superposition State of an Atom. *Science* **272**, 1131 (1996).

[2] M. Brune, E. Hagley, J. Dreyer, X. Maître, A. Maali, C. Wunderlich, J. M. Raimond, and S. Haroche. Observing the Progressive Decoherence of the "Meter" in a Quantum Measurement. *Phys. Rev. Lett.* **77**, 4887 (1996).

[3] *The Nobel Prize in Physics 2012 - Advanced Information.* Nobelprize.org. 17 Nov 2012, www.nobelprize.org/nobel_prizes/physics/laureates/2012/advanced.html

[4] A. Blais, R. S. Huang, A. Wallraff, S. M. Girvin, and R. J. Schoelkopf. Cavity quantum electrodynamics for superconducting electrical circuits: An architecture for quantum computation. *Phys. Rev. A* **69**, 062320 (2004).

[5] A. Wallraff, D. I. Schuster, A. Blais, L. Frunzio, R.-S. Huang, J. Majer, S. Kumar, S. M. Girvin, and R. J. Shoelkopf. Strong coupling of a single photon to a superconducting qubit using circuit quantum electrodynamics. *Nature* **431**, 162 (2004).

[6] R. P. Feynman. Simulating Physics with Computers. *International Journal of Theoretical Physics* **21**, 467 (1982).

[7] D. Deutsch. Quantum Theory, the Church-Turing Principle and the Universal Quantum Computer. *Proc. R. Soc. Lond. A* **400**, 97 (1985).

[8] P. W. Shor. Polynomial-Time Algorithms for Prime Factorization and Discrete Logarithms on a Quantum Computer. *Proceedings of the 35th Annual Symposium on Foundations of Computer Science*, 124 (1995).

[9] L. K. Grover. Quantum Mechanics Helps in Searching for a Needle in a Haystack. *Phys. Rev. Lett.* **79**, 325 (1997).

[10] A. W. Harrow, A. Hassidim, and S. Lloyd. Quantum Algorithm for Linear Systems of Equations. *Phys. Rev. Lett.* **103**, 150502 (2009).

[11] M. A. Nielsen and I. L. Chuang. *Quantum Computation and Quantum Information*, Cambridge University Press, Cambridge (2000).

[12] H. Paik, D. I. Schuster, L. S. Bishop, G. Kirchmair, G. Catelani, A. P. Sears, B. R. Johnson, M. J. Reagor, L. Frunzio, L. I. Glazman, S. M. Girvin, M. H. Devoret, and R. J. Schoelkopf. Observation of High Coherence in Josephson Junction Qubits Measured in a Three-Dimensional Circuit QED Architecture. *Phys. Rev. Lett.* **107**, 240501 (2011).

[13] S. B. Bravyi and A. Y. Kitaev. Quantum codes on a lattice with boundary. ArXiv preprint: arxiv.org/abs/arXiv:quant-ph/9811052 (1998).

[14] A. G. Fowler, M. Mariantoni, J. M. Martinis, and A. N. Cleland. Surface codes: Towards practical large-scale quantum computation. *Phys. Rev. A* **86**, 032324 (2012).

[15] K. Lalumiere, J. M. Gambetta, and A. Blais. Tunable joint measurements in the dispersive regime of cavity QED. *Phys. Rev. A* **81**, 040301(R) (2010).

[16] H. M. Wiseman and G. J. Milburn. *Quantum Measurement and Control*, Cambridge University Press, Cambridge (2010).

[17] J. Gough and M. R. James. Quantum Feedback Networks: Hamiltonian Formulation. *Commun. Math. Phys.* **287**, 1109 (2009).

[18] J. Gough and M. R. James. The Series Product and Its Application to Quantum Feedforward and Feedback Networks. *IEEE Transactions on Automatic Control* **54**, 2530 (2009).

[19] B. Q. Baragiola, R. L. Cook, A. M. Brańczyk, and J. Combes. *N*-photon wave packets interacting with an arbitrary quantum system. *Phys. Rev. A* **86**, 013811 (2012).

[20] Observation of Quantum Jumps in a Single Atom. J. C. Bergquist, R. G. Hulet, W. M. Itano, and D. J. Wineland. *Phys. Rev. Lett.* **57**, 1699 (1986).

[21] J. I. Cirac and P. Zoller. Quantum Computations with Cold Trapped Ions. *Phys. Rev. Lett.* **74**, 4091 (1995).

[22] H. Häffner, W. Hänsel, C. F. Roos, J. Benhelm, D. Chek-al-kar, M. Chwalla, T. Körber, U. D. Rapol, M. Riebe, P. O. Schmidt, C. Becher, O. Gühne, W. Dür, and R. Blatt. Scalable multiparticle entanglement of trapped ions. *Nature* **438**, 643 (2005).

[23] C. Guerlin, J. Bernu, S. Deléglise, C. Sayrin, S. Gleyzes, S. Kuhr, M. Brune, J. M. Raimond, and S. Haroche. Progressive field-state collapse and quantum non-demolition photon counting. *Nature* **448**, 889 (2007).

[24] R. Miller, T.E. Northup, K.M. Birnbaum, A. Boca, A.D. Boozer and H.J. Kimble. Trapped atoms in cavity QED: coupling quantized light and matter. *J. Phys. B* **38**, S551 (2005).

[25] H. Walther, B. T. H. Varcoe, B.-G. Englert, and T. Becker. Cavity quantum electrodynamics. *Rep. Prog. Phys.* **69**, 1325 (2006).

[26] R. J. Schoelkopf and S. M. Girvin. Wiring up quantum systems. *Nature* **451**, 664 (2008).

[27] C. M. Wilson, G. Johansson, A. Pourkabirian, M. Simoen, J. R. Johansson, T. Duty, F. Nori, and P. Delsing. Observation of the dynamical Casimir effect in a superconducting circuit. *Nature* **479**, 376 (2011).

[28] L. S. Bishop, J. M. Chow, J. Koch, A. A. Houck, M. H. Devoret, E. Thuneberg, S. M. Girvin, and R. J. Schoelkopf. Nonlinear response of the vacuum Rabi resonance. *Nature Physics* **5**, 105 (2009).

[29] J. M. Fink, R. Bianchetti, M. Baur, M. Göppl, L. Steffen, S. Filipp, P. J. Leek, A. Blais, and A. Wallraff. Dressed Collective Qubit States and the Tavis-Cummings Model in Circuit QED. *Phys. Rev. Lett.* **103**, 083601 (2009).

[30] B. Yurke and J. S. Denker. Quantum Network Theory. *Phys. Rev. A* **29**, 1419 (1984).

[31] M. H. Devoret. Quantum fluctuations in electrical circuits, in *Quantum Fluctuations: Les Houches Session LXIII*, Eds. S. Reynaud, E. Giacobino, and J. Zinn-Justin (1997).

[32] L. Tornberg. *Superconducting qubits - measurement, entanglement, and noise.* Ph. D. Gothenburg: Chalmers University of Technology (2009).

[33] J. R. Johansson. *Quantum mechanics in superconducting circuits and nanomechanical devices.* Ph. D. Gothenburg: Chalmers University of Technology (2009).

[34] L. S. Bishop. *Circuit Quantum Electrodynamics.* Ph.D. New Haven: Yale University (2010).

[35] D. M. Pozar. *Microwave Engineering*, 3rd ed., John Wiley & Sons, Inc. (2005).

[36] R. E. Collin. *Foundations for Microwave Engineering*, 2nd ed., Wiley-IEEE Press (2001).

[37] H. Goldstein. *Classical Mechanics*, 2nd ed., Addison-Wesley Publishing Company, Inc., Reading (1980).

[38] J. J. Sakurai. *Modern Quantum Mechanics*, Revised ed., Addison-Wesley Publishing Company, Inc., Reading (1994).

[39] M. E. Peskin and D. V. Schroeder. *An Introduction to Quantum Field Theory*, Westview Press, Boulder (1995).

[40] J. M. Martinis, M. H. Devoret, and J. Clarke. Energy-Level Quantization in the Zero-Voltage State of a Current-Biased Josephson Junction. *Phys. Rev. Lett.* **55**, 1543 (1985).

[41] Y. Makhlin, G. Schön, and A. Shnirman. Josephson-junction qubits with controlled couplings. *Nature* **398**, 305 (1999).

[42] Y. Nakamura, Y. A. Pashkin, and J. S. Tsai. Coherent control of macroscopic quantum states in a single-Cooper-pair box. *Nature* **398**, 786 (1999).

[43] D. Vion, A. Aassime, A. Cottet, P. Joyez, H. Pothier, C. Urbina, D. Esteve, and M. H. Devoret. Manipulating the Quantum State of an Electrical Circuit. *Science* **296**, 886 (2002).

[44] J. Clarke and F. K. Wilhelm. Superconducting quantum bits. *Nature* **453**, 1031 (2008).

[45] V. E. Manucharyan, J. Koch, L. I. Glazman, M. H. Devoret. Fluxonium: Single Cooper-Pair Circuit Free of Charge Offsets. *Science* **326**, 113 (2009).

[46] B. D. Josephson. Possible new effects in superconductive tunnelling. *Phys. Lett.* **1**, 251 (1962).

[47] J. R. Waldram. *Superconductivity of metals and cuprates*, IOP Publishing Ltd, London (1996).

[48] J. Koch, T. M. Yu, J. Gambetta, A. A. Houck, D. I. Schuster, J. Majer, A. Blais, M. H. Devoret, S. M. Girvin, and R. J. Schoelkopf. Charge-insensitive qubit design derived from the Cooper pair box. *Phys. Rev. A* **76**, 042319 (2007).

[49] I.-C. Hoi, C.M. Wilson, G. Johansson, T. Palomaki, B. Peropadre, and P. Delsing. Demonstration of a Single-Photon Router in the Microwave Regime. *Phys. Rev. Lett.* **107**, 073601 (2011).

[50] M. D. Reed, L. DiCarlo, S. E. Nigg, L. Sun, L. Frunzio, S. M. Girvin, and R. J. Schoelkopf. Realization of three-qubit quantum error correction with superconducting circuits. *Nature* **482**, 382 (2012).

[51] C. C. Gerry and P. L. Knight. *Introductory Quantum Optics*, Cambridge University Press, Cambridge (2005).

[52] L. DiCarlo, M. D. Reed, L. Sun, B. R. Johnson, J. M. Chow, J. M. Gambetta, L. Frunzio, S. M. Girvin, M. H. Devoret, and R. J. Schoelkopf. Preparation and measurement of three-qubit entanglement in a superconducting circuit. *Nature* **467**, 574 (2010).

[53] I. I. Rabi. Space Quantization in a Gyrating Magnetic Field. *Phys. Rev.* **51**, 652 (1937).

[54] E. T. Jaynes and F. W. Cummings. Comparison of Quantum and Semiclassical Radiation Theories with Application to the Beam Maser. *Proc. IEEE* **51**, 89 (1963).

[55] M. Tavis and F. W. Cummings. Exact Solution for an N-Molecule-Radiation-Field Hamiltonian. *Phys. Rev.* **170**, 379 (1968).

[56] M. Boissonneault, J. M. Gambetta, and A. Blais. Dispersive regime of circuit QED: Photon-dependent qubit dephasing and relaxation rates. *Phys. Rev. A* **79**, 013819 (2009).

[57] N. Boulant, G. Ithier, P. Meeson, F. Nguyen, D. Vion, D. Esteve, I. Siddiqi, R. Vijay, C. Rigetti, F. Pierre, and M. Devoret. Quantum nondemolition readout using a Josephson bifurcation amplifier. *Phys. Rev. B.* **76**, 014525 (2007).

[58] B. R. Johnson, M. D. Reed, A. A. Houck, D. I. Schuster, Lev S. Bishop, E. Ginossar, J. M. Gambetta, L. DiCarlo, L. Frunzio, S. M. Girvin, and R. J. Schoelkopf. Quantum non-demolition detection of single microwave photons in a circuit. *Nature Physics* **6**, 663 (2010).

[59] H. J. Carmichael. *An Open Systems Approach to Quantum Optics*, Springer-Verlag, New York (1993).

[60] H. -P. Breuer and F. Petruccione. *The theory of Open Quantum Systems*, Oxford University Press, Oxford (2002).

[61] C.W. Gardiner and P. Zoller. *Quantum Noise*, Springer-Verlag, Berlin, Heidelberg (1991).

[62] G. Lindblad. On the Generators of Quantum Dynamical Semigroups. *Comm. Math. Phys.* **48**, 119 (1976).

[63] C. W. Gardiner and M. J. Collett. Input and output in damped quantum systems: Quantum stochastic differential equations and the master equation. *Phys. Rev. A* **31**, 3761 (1985).

[64] H. J. Carmichael. Quantum Trajectory Theory for Cascaded Open Systems. *Phys. Rev. Lett.* **70**, 2273 (1993).

[65] H. M. Wiseman. *Quantum Trajectories and Feedback.* Ph.D. Brisbane: University of Queensland (1994).

[66] R. L. Hudson and K. R. Parthasarathy. Quantum Itō's Formula and Stochastic Evolutions. *Commun. Math. Phys.* **93**, 301 (1984).

[67] An introduction to quantum filtering. L. Bouten, R. van Handel, and M. R. James. *SIAM J. Control Optim.* **46**, 2199 (2007).

[68] J. Kerckhoff. *Quantum Engineering with Quantum Optics*. Ph.D. Stanford: Stanford University (2011).

[69] M.P. da Silva, D. Bozyigit, A. Wallraff, and A. Blais. Schemes for the observation of photon correlation functions in circuit QED with linear detectors. *Phys. Rev. A* **82**, 043804 (2010).

[70] N. Tezak, A. Niederberger, D. S. Pavlichin, G. Sarma, and H. Mabuchi. Specification of photonic circuits using Quantum Hardware Description Language. *Phil. Trans. Roy. Soc. A* **370**, 5270 (2012).

[71] K. M. Gheri, K. Ellinger, T. Pellizzari, and P. Zoller. Photon-Wavepackets as Flying Quantum Bits. *Fortschr. Phys.* **46**, 401 (1998).

[72] J. E. Gough, M. R. James, H. I. Nurdin, and J. Combes. Quantum filtering for systems driven by fields in single-photon states or super-position of coherent states. *Phys. Rev. A* **86**, 043819 (2012).

[73] R. Loudon. *The Quantum Theory of Light*, 3rd ed., Oxford University Press, Oxford (2000).

[74] J. E. Gough, M. R. James, and H. I. Nurdin. Quantum Master Equation and Filter for Systems Driven by Fields in a Single Photon State ArXiv preprint: arxiv.org/abs/1107.2973 (2011).

[75] Y. Wang, J. Minar, L. Sheridan, and V. Scarani. Efficient excitation of a two-level atom by a single photon in a propagating mode. *Phys. Rev. A* **83**, 063842 (2011).

[76] L. Tornberg and G. Johansson. High-fidelity feedback-assisted parity measurement in circuit QED. *Phys. Rev. A* **82**, 012329 (2010).

[77] J. Gambetta, A. Blais, M. Boissonneault, A. A. Houck, D. I. Schuster, and S. M. Girvin. Quantum trajectory approach to circuit QED: Quantum jumps and the Zeno effect. *Phys. Rev. A* **77**, 012112 (2008).

[78] Y.-F. Chen, D. Hover, S. Sendelbach, L. Maurer, S. T. Merkel, E. J. Pritchett, F. K. Wilhelm, and R. McDermott. Microwave Photon Counter Based on Josephson Junctions. *Phys. Rev. Lett.* **107**, 217401 (2011)

[79] G. Romero, J. J. Garcia-Ripoll, and E. Solano. Microwave Photon Detector in Circuit QED. *Phys. Rev. Lett.* **102**, 173602 (2009).

[80] B. Peropadre, G. Romero, G. Johansson, C. M. Wilson, E. Solano, and J. J. Garcia-Ripoll. Approaching perfect microwave photodetection in circuit QED. *Phys. Rev. A* **84**, 063834 (2011).

[81] J.R. Johansson, P.D. Nation, and F. Nori. QuTiP: An open-source Python framework for the dynamics of open quantum systems. *Comp. Phys. Com.* **183**, 1760 (2012).

[82] A. C. Doherty, S. Habib, K. Jacobs, H. Mabuchi, and S. M. Tan. Quantum feedback control and classical control theory. *Phys. Rev. A* **62**, 012105 (2000).

[83] L. Bouten, R. van Handel, and M. James. A discrete invitation to quantum filtering and feedback control. *SIAM Review* **51**, 239 (2009).

[84] J. Kerckhoff, H. Nurdin, D. S. Pavlichin, and H. Mabuchi. Designing quantum memories with embedded control: photonic circuits for autonomous quantum error correction *Phys. Rev. Lett.* **105**, 040502 (2010).

[85] J. Kerckhoff, D. S. Pavlichin, H. Chalabi, and H. Mabuchi. Design of nanophotonic circuits for autonomous subsystem quantum error correction. *New J. Phys.* **13**, 055022 (2011).

[86] J. Koch, A. A. Houck, K. Le Hur, and S. M. Girvin. Time-reversal-symmetry breaking in circuit-QED-based photon lattices. *Phys. Rev. A* **82**, 043811 (2010).